npj | Climate and Atmospheric Science

www.nature.com/npjclimatsci

REVIEW ARTICLE OPEN

Check for updates

Formation of secondary organic aerosols from anthropogenic precursors in laboratory studies

Deepchandra Srivastava[1], Tuan V. Vu[2], Shengrui Tong[3], Zongbo Shi[1] and Roy M. Harrison[1,4]✉

Aerosols produced from the oxidation of volatile/semi-volatile organic compounds (VOCs/SVOCs), known as secondary organic aerosol (SOA), account for a significant fraction of atmospheric airborne particles. This paper reviews the current understanding of SOA formation from gas-phase oxidation with a focus on anthropogenic precursors and their reaction products from atmospheric simulation chamber studies. The review summarises the major reaction products derived from main groups of SOA precursors (e.g., alkanes, aromatics), SOA yields and the factors controlling SOA formation. We highlight that lab-derived SOA yield depends strongly upon, not only the concentrations of SOA precursors and oxidants but also simulation conditions.

npj Climate and Atmospheric Science (2022)5:22 ; https://doi.org/10.1038/s41612-022-00238-6

INTRODUCTION

Atmospheric aerosols significantly affect visibility, air quality and climate[1]. Exposure to atmospheric aerosols has been associated with increased cardiopulmonary mortality and morbidity[2]. Atmospheric organic aerosols (OAs) may originate from natural and anthropogenic sources and account for 20–50% of aerosol loading globally[3,4]. The composition of OAs may be complex, comprising of thousands of compounds from simple hydrocarbons to highly oxidized compounds. Directly emitted hydrocarbon components are referred to as primary organic aerosols (POAs) and OA formed via the atmospheric oxidation of volatile and semi-volatile organic compounds (VOCs) are referred to as secondary organic aerosol (SOA).

The formation of SOAs has recently received much attention as they have been shown to be a major component of atmospheric OAs[5]. For example, 50% of fine particle mass is composed of OAs in the urban locations within the Northern Hemisphere. The SOA fraction ranged from 65 to 95% between urban and remote regions[6]. The precursors of SOAs include VOCs emitted from both biogenic (e.g., terrestrial vegetation, grassland, peatlands and forest) and anthropogenic sources (e.g., biomass burning, coal combustion, transportation, solvent utilization and industry). Under atmospheric conditions, VOCs may undergo atmospheric oxidation with ozone (O_3), nitrate (NO_3) and hydroxyl radicals (OH) to form less volatile products which may undergo further reactions and/or partition into the condensed phase, leading to complex chemical composition profiles within the aerosol.

Atmospheric models indicate that annual SOA fluxes are largely dominated by biogenic SOA (BSOA, 88 TgC/yr), followed by biomass burning SOA (BBSOA, 17 TgC/yr), and anthropogenic SOA (ASOA, 10 TgC/yr)[7]. This highlights the dominance of biogenic VOCs over other SOA precursors, where isoprene alone contributes ~50% to the global VOCs flux[8]. ASOA precursors are mostly composed of alkanes (40%), followed by aromatics (20%) and alkenes (10%) with the rest being oxygenated and unidentified compounds[9]. In urban environments, light aromatic hydrocarbons contribute up to 30% of VOCs[10] and 3–25 TgC/yr to global SOA production, up to 2–3 fold higher than previous model estimates[11]. Ambient measurements have also shown the importance of ASOA in urban environments as they were found to be contributing significantly to the OA mass and can be substantially higher in concentration than BSOA[12,13].

Atmospheric models use parameterizations of SOA yield curves obtained from laboratory experiments to predict SOA mass concentrations. However, SOA yield data are not available for all ASOA precursors due to a limited number of laboratory studies, with some ASOA precursors and processes (e.g., cloud processing or other aerosol-phase reactions) that contribute to SOA not being considered[14]. OAs need to be well characterised within atmospheric models to develop effective air quality management plans, that mitigate adverse health and climate impacts of atmospheric aerosol loading and exposure. There are several potential causes for the widespread negative bias in model predictions of OAs. This review focuses on SOA formation from ASOA precursors, which historically has not been investigated extensively.

The objectives of this work are to summarize the outcomes of existing knowledge on ASOA precursors and their oxidation products from atmospheric simulation chamber studies. We also compare SOA yields from different precursors and the factors controlling the SOA mass yield. Since this is a very large subject, the coverage does not extend to natural precursors such as isoprene and terpenes, or to reaction processes in the aqueous phase. The latter have been reviewed by Blando and Turpin[15], Carlton et al.[16], Ervens et al.[17] and Mahilang et al.[18] Finally, gaps in knowledge between SOA contribution from lab, field and modelling studies are discussed.

LABORATORY EXPERIMENTS

SOA-forming potentials of precursors are generally estimated through atmospheric simulation chamber experiments to derive a yield. A brief description of their design is presented hereafter.

[1]Division of Environmental Health & Risk Management, School of Geography, Earth & Environmental Sciences, University of Birmingham, Edgbaston, Birmingham B15 2TT, UK. [2]Faculty of Medicine, School of Public Health, Imperial College London, London, UK. [3]State Key Laboratory for Structural Chemistry of Unstable and Stable Species Institute of Chemistry, Chinese Academy of Sciences Zhongguancun, Beijing 100190, P. R. China. [4]Department of Environmental Sciences/Center of Excellence in Environmental Studies, King Abdulaziz University, PO Box 80203, Jeddah 21589, Saudi Arabia. ✉email: r.m.harrison@bham.ac.uk

Published in partnership with CECCR at King Abdulaziz University

npj nature partner journals

Smog chamber/ potential aerosol mass (PAM) designs

Smog (environmental) chamber designs. Predominantly, chambers are several cubic metres in volume and made from Teflon film and are often equipped with a standard set of instruments, including an integrated temperature and humidity probe and a differential pressure indicator[19–22]. In addition, chambers are often equipped with sets of narrow-band blacklights and/or UV broad-band lamps for irradiation[20,21]. The lamps usually have a standard $300-400$ nm spectrum, centred at 350 nm. Different light intensities can be used depending on the experimental requirements (e.g., high or low nitrogen oxides (NO_x))[23].

In most high-NO_x experiments, OH radicals are produced by the photolysis of nitrous acid (HONO) using UV lamps[24–27]. Even though NO_x is produced from HONO photolysis, additional NO can be added to the chamber to reach the desired VOC/ NO_x ratios.

For low-NO_x experiments, H_2O_2 is used as the OH precursor[25,28]. An atmospherically relevant OH concentration (ca.10^6 molecule cm^{-3}) is produced by photolysing the H_2O_2 in the chamber[29–31]. OH radicals can also be generated by photolysis of isopropyl/ methyl nitrite. (Reactions: 1–3) when added into the chamber[32,33].

$$(CH_3)_2CHONO/CH_3NO + h\nu \rightarrow (CH_3)_2CHO/CH_3 + NO \quad (1)$$

$$(CH_3)_2CHO/CH_3 + O_2 \rightarrow CH_3COCH_3/CH_2 + HO_2 \quad (2)$$

$$HO_2 + NO \rightarrow OH + NO_2 \quad (3)$$

Oxidation flow reactor (OFR) designs. Oxidation Flow Reactors (OFRs) produce highly oxidizing conditions to accelerate processes which would usually take a number of days in the atmosphere to a few minutes in the laboratory/field. In addition to being used to generate SOA particles, the OFRs are also used to simulate atmospheric processing of soot and other model POAs. OFR185 and OFR254 (i.e., 185 and 254 nm photolysis lamps) are the most basic operation modes and have been used most widely to investigate the accelerated atmospheric chemistry[34]. In OFR254 mode, filtered low-pressure mercury lamps provide 254 nm light to photolyze externally generated O_3 in the reactor to form OH (Reactions: 4–5). However, in OFR185 mode the low-pressure mercury lamps are not filtered and emit 185 nm light that can photolyze H_2O producing OH, and O_2 into $O(^3P)$, meaning externally generated O_3 is not required. In addition, $O(^3P)$ recombines with O_2 to form O_3, which can also produce OH with the help of 254 nm UV lamps, as in OFR254. Hence, OH radical ($8\times10^8-2\times10^{10}$ molecule cm^{-3}) production processes for both, OFR254 and OFR185, is given by Reactions: 4–5 and 6–9, respectively[34–37]. OFRs are operated under continuous flow conditions, where environmental chambers are typically run in batches. The OH/HO_2 and OH/O_3 ratios in the OFRs are similar to those found in the troposphere, while daytime concentrations of OH, HO_2 and O_3 are 100 to 10,000 times larger.

For OFR254

$$O_3 + h\nu(\lambda = 254nm) \rightarrow O_2 + O(^1D) \quad (4)$$

$$O(^1D) + H_2O \rightarrow 2OH \quad (5)$$

For OFR185

$$H_2O + O_2 + h\nu(\lambda = 185nm) \rightarrow \rightarrow OH + HO_2 \quad (6)$$

$$3O_2 + h\nu(\lambda = 185nm) \rightarrow\rightarrow 2O_3 \quad (7)$$

$$O_3 + h\nu(\lambda = 254nm) \rightarrow O_2 + O(^1D) \quad (8)$$

$$O(^1D) + H_2O \rightarrow 2OH \quad (9)$$

*Two consecutive arrows represent that some basic steps are ignored.

The Potential Aerosol Mass (PAM) reactor is the most popular OFR to study oxidation chemistry, and only one is available commercially (from Aerodyne Research, Inc., Billerica, MA, USA). The reactor is cylindrical (internal diameter ~ 20 cm and volume ~ 10 L) with a residence time of usually 100–200 s[34]. The role of OFRs in atmospheric chemistry research has already been reviewed by Peng and Jimenez[34].

Analytical methods for SOA composition (tracers)

To identify and quantify the chemical composition of SOA, a wide range of online (i.e. CIMS (chemical ionisation mass spectrometry), HR-ToF-AMS (high-resolution time of flight aerosol mass spectrometry))[38,39] and off-line (i.e. GC/MS, 2D-GC/ToF-MS) techniques have been used in recent decades. In terms of off-line measurements, SOA products are collected on filters (Quartz or PTFE filters) and then go directly for analysis using thermal desorption-GCxGC-ToF/MS techniques[40], or the collected filters can be extracted, derivatised and then analysed by GC/MS or 2D-GC-ToF/MS techniques[41].

SOA FORMATION PATHWAYS AND REACTION PRODUCTS

This section reviews the reaction products observed from the oxidation of AVOCs. Details on the reaction products from alkane and aromatic AVOC oxidation are given in Tables 1 and 2. Most studies have involved single precursor VOC, but many have varied the concentrations of NO_x, which can fundamentally influence reaction pathways, and have included seed inorganic or organic aerosol, both of which influence SOA yields. The mechanisms and effects of such additional factors are explored in later sections. Overall, this section begins with providing a short description of alkanes and aromatics, and their relevance in the atmosphere, followed by a generalised reaction scheme based on the oxidation from OH, chlorine (Cl) and nitrate (NO_3) radical. Later, the section discusses major reaction products obtained from the oxidation of individual precursors under different experimental conditions based on the results from published studies. In addition, a brief introduction to organosulfates formation from the oxidation of alkanes and aromatics is also included.

Alkanes and alkyl groups

Alkanes are a main class of AVOCs (40–50% of total VOCs) in urban areas[32,42]. They are predominantly emitted from combustion sources, such as traffic emissions, petroleum and fossil fuel combustion[31]. Ensberg et al.[43] reported that a major fraction of diesel and gasoline fuels contains cyclic, branched and linear alkanes, while long-chain alkanes constitute a substantial fraction of the unresolved complex mixture from fossil fuels[44]. Their ambient lifetimes are predominantly governed by reaction with OH and range from 0.5 days for *n*-hexadecane (C_{16}) to 1.4 days for *n*-octane (C_8)[45,46]. This is sufficiently long for their transport from urban to rural areas, indicating their importance within the atmosphere. Therefore, following the development sequence, the generalised alkane oxidation reaction scheme (SOA formation pathways) and the oxidation products are discussed below.

Formation pathways. In the atmosphere, OH is the dominant daytime sink of alkanes forming alkyl peroxy radicals (RO_2). RO_2 subsequently reacts with NO to form alkyl nitrate or alkoxy radicals (RO), which could react with O_2, decompose or isomerize[23,33]. The reaction mechanism of OH with linear, branched, or cyclic alkanes in the presence of NO_x is shown in Fig. 1. For linear and branched alkanes, decomposition leads to fragmentation and forms carbonyls and RO_2 after addition of O_2. For cyclic alkanes, the formation of a single ring-opened carbonyl RO_2 is observed. All RO_2 formed at different stages (alkyl peroxy, carbonyl alkyl peroxy, and 1,4-hydroxy alkyl peroxy radicals) can react further with NO/ O_2 or isomerise or react again with OH radicals to form multigeneration products.

Table 1. Aliphatic precursors and reaction products.

Alkanes-precursors	Experimental conditions	Reaction products	References
$C_{8–15}$ alkanes	Chamber-based high NO_x, OH oxidation	Hydroxy nitrates, dinitrates, and substituted tetrahydrofurans	Lim and Ziemann[21]
C_5–C_8 alkanes	Chamber-OH oxidation with NO	Hydroxy ketones	Reisen et al.[49]
$C_{15,16}$ n-alkanes	Chamber-based high NO_x, OH oxidation	Dihydrofurans, alkyl nitrates, and hydroxy ketones	Lim and Ziemann[22]
$C_{6–17}$ linear alkanes, C_{6-11} branched alkanes, $C_{6-8,10,12,15}$ cyclic alkanes	Chamber-based high NO_x, OH oxidation	Dihydrofurans, alkyl nitrates, and hydroxy ketones	Lim and Ziemann[33]
C_{10} alkanes	Chamber, Cl	Decanal, decyl alcohol, heptaldehyde, heptyl alcohol, and hexyl alcohol	Shi et al.[96]
C_{10}–C_{12} alkanes	Chamber, high NO_x, Cl, dry/humid	Organonitrates (hydroxy nitrates, $ONO_2{-}C_nH_{2n+1}O$; oxidized organonitrates, $ONO_2{-}C_nH_{2n-5}O_4$), $C_2H_3ClO_2$ and $C_2H_2Cl_2O_2$	Wang and Hildebrandt Ruiz[94]
	Outdoor smog chamber	**$C_7H_{15}O_4S$–, $C_{10}H_{17}O_5S$–, $C_9H_{19}O_6S$–, $C_{10}H_{19}O_6S$–, $C_{10}H_{17}O_7S$–, $C_{10}H_{19}O_8S$–, $C_{12}H_{19}O_7S$–, and $C_{10}H_{15}O_9S$–**	Riva et al.[128]
C_{11} alkanes	Chamber, Cl	Heptaldehyde, butyraldehyde, heptyl alcohol, octanal, hexyl alcohol, 1-hydroxy-butanone, 1-octanol, 1-hydroxy-propanone, 1-hydroxy-pentanone and 1-hydroxy-hexanone	Shi et al.[96]
C_{12} alkanes	Chamber-based OH oxidation	Hydroxycarbonyls, hydroperoxycarbonyls, hydroperoxides, peracids, and PHA	Craven et al.[51]
	Chamber-based OH oxidation, low-NO_x	Hydroxycarbonyls, hydroperoxides, hydroperoxycarbonyls, hydroxy hydroperoxides, peracids, PHA, and dihydroperoxides	Yee et al.[50]
	Chamber-OH oxidation, low-NO_x /high-NO_x	Hydroxycarbonyls, and dihydrofurans	Zhang et al.[55]
	Chamber-OH oxidation, low-NO_x	Hydroperoxides, hydroxycarbonyls, PHA, and hemiacetals	Fahnestock et al.[31]
	Chamber-OH oxidation, high-NO_x	Alcohols, aldehydes, hemiacetals, nitrate-bearing hemiacetals, and acid anhydrides	Fahnestock et al.[31]
	Chamber-based OH oxidation	Hydroxycarbonyls, hydroperoxides, hydroperoxy carbonyls, acids, and PHA	Yee et al.[52]
	Smog chamber, OH, high NO_x	Hydroxycarbonyls, hemiacetals, and acid anhydrides	Li et al.[56]
	Chamber, Cl	Octanal, hexanal, propionaldehyde, hexyl alcohol, 1-hydroxy-propanone, 1- hydroxy-butanone, 1-hydroxy-pentanone and 1-hydroxy-hexanone	Shi et al.[96]
C_{13} alkanes	Chamber, Cl	Acetaldehyde, propionaldehyde, butyraldehyde, valeraldehyde, hexanal, hexyl alcohol, heptaldehyde and 1-hydroxy-butanone	Shi et al.[96]
C_{14} alkanes	Chamber, Cl	Heptaldehyde, butyraldehyde, hexanal, acetaldehyde, propionaldehyde, hexyl alcohol, 1- hydroxy-propanone, heptyl alcohol, 1-hydroxy-butanone and octanal	Shi et al.[96]
$C_{15,}$ C_{17} alkanes	Smog chamber, OH, high NO_x	Hydroxycarbonyls, hemiacetals, and acid anhydrides	Li et al.[56]
C_{10}–C_{17} alkanes	Chamber-OH oxidation, NO_x	Cyclic hemiacetal, hemiacetal nitrate and hemiacetal dinitrates	Docherty et al.[57]
2-Methylundecane	Chamber-based OH oxidation	Hydroxycarbonyls, hydroperoxides, hydroperoxy carbonyls, acids, and PHA	Yee et al.[52]
Cholestane ($C_{27}H_{48}$)	FTR, OH-heterogeneous oxidation	Ketones, aldehydes, alcohols, and hydroxy ketones	Zhang et al.[54]
Squalane ($C_{30}H_{62}$), octacosane	FTR, OH-heterogeneous oxidation	Carbonyls, alcohols, lactones, hydroxy ketones, and carboxylic acids	Ruehl et al.[48]
2,6,10-Trimethyldodecane	Chamber-based high NO_x, OH oxidation	Dihydrofurans, alkyl nitrates, and hydroxy ketones	Lim and Ziemann[22]
$C_{6,7,8,10}$ cyclic monoalkenes	Chamber-based ozonolysis	Alkoxyhydroperoxy aldehydes, and PHA	Ziemann[53]
$C_{12–15}$ cyclic alkanes	Chamber-based high NO_x, OH oxidation	Dihydrofurans, alkyl nitrates, and hydroxy ketones	Lim and Ziemann[22]
$C_{6–8,10,12,15}$ cyclic alkanes	Chamber-based high NO_x, OH oxidation	Dihydrofurans, alkyl nitrates, and hydroxy ketones	Lim and Ziemann[33]

Table 1 continued

Alkanes-precursors	Experimental conditions	Reaction products	References
Cyclododecane	Chamber-OH oxidation, low- NO_x	Ethers, PHA, hydroxycarbonyls, alcohols, and hydroperoxides	Fahnestock et al.[31]
	Chamber-OH oxidation, high- NO_x	Ethers, esters, hydroxycarbonyls, alcohols, and nitrates	Fahnestock et al.[31]
	Chamber-based OH oxidation	Hydroxycarbonyls, hydroperoxides, hydroperoxy carbonyls, acids, and PHA	Yee et al.[52]
Hexylcyclohexane	Chamber-OH oxidation, low- NO_x	Hydroperoxides, PHA, hemiacetals, and hydroxycarbonyls	Fahnestock et al.[31]
	Chamber-OH oxidation, high- NO_x	Hydroxycarbonyl dimers, hemiacetals, and esters (with nitrate/imine groups)	Fahnestock et al.[31]
	Chamber-based OH oxidation	Hydroxycarbonyls, hydroperoxides, hydroperoxy carbonyls, acids, and PHA	Yee et al.[52]
C_{6-11} branched alkanes	Chamber-based high NO_x, OH oxidation	Dihydrofurans, alkyl nitrates, and hydroxy ketones	Lim and Ziemann[33]

*Bold: SOA tracer.

Major reaction products. A wide range of SOA products have been identified, which not only strongly depend on molecular size and structure of each precursor (linear/ branched/cyclic and functional groups) and degree of oxidation, but also on other chamber conditions during the ageing process (i.e., NO_x concentration and relative humidity (RH))[47,48]. Alcohols, carboxylic acids, ketones and carbonyls are commonly the first oxidation products of branched and linear alkanes[22,48,49]. Carbonyls are predominantly formed from reactions of OH and C_5-C_8 *n*-alkanes with NO[49]. Reisen et al.[49] found that formation of 1,4-hydroxycarbonyls accounts for 54, 57, 51, and 53% of the reaction products from C_5-C_8 *n*-alkanes, respectively. The formation of relatively more complex structures occurs as second phase oxidation products come from the aerosol chemistry of carbonyl groups. For example, 1,4-substituted hydroxycarbonyl compounds may undergo cyclization and result in the formation of cyclic hemiacetals that can dehydrate to form highly reactive substituted dihydrofurans or aldehydes that undergo imine formation with amines.

OH-initiated reactions of *n*-dodecane (C_{12})/2-methylundecane/ hexylcyclohexane and cyclododecane with low-NO_x result in the formation of the RO_2 radical that rapidly produces a hydroperoxide upon reaction with HO_2 as a first-generation product, and subsequently several high generation products, such as hydroxycarbonyls, hydroperoxides, hydroperoxycarbonyls, hydroxy hydroperoxides, peracids, peroxyhemiacetals (PHA), and dihydroperoxide[31,50–52]. It has also been reported that acidic species are expected to form from the photolysis of hydroperoxy groups which include carboxylic acids, peracids, hydroxy carboxylic acids, and hydroxy peracids. It was also reported that the dominant species in *n*-dodecane SOA formed under low-NO conditions are functionalized hemiacetals and peroxyhemiacetals, which account for 98% of the estimated SOA mass[31]. They are formed from aerosol chemistry traditionally considered to be acid-catalysed. In addition, low-NO_x SOA formed from cyclododecane is mainly composed of ethers and peroxyhemiacetals and contains minor contributions of hydroxycarbonyls, hydroperoxides, and alcohols. Similarly, hexylcyclohexane SOA is composed of hydroperoxides, peroxyhemiacetals, hemiacetals, and hydroxycarbonyls under low-NO_x conditions.

Under high NO_x, more SOA products are identified, such as nitrate and ester groups[44]. The formation of hydroxy-nitrates, dinitrates, and alkyl nitrates are observed by oxidation of alkanes (C_6-C_{15}) with OH under high concentration of NO_x[21,22,33]. The oxidation products formed from the reactions of OH with linear, branched, and cyclic alkanes are similar. The first-generation SOA products rapidly isomerize in the aerosol phase to form cyclic hemiacetals, which go on to dehydrate to form volatile dihydrofurans. Any volatile products react with OH forming multigeneration products, which are acyclic or monocyclic for all alkanes, and can also be bicyclic from cyclic alkanes. In addition, 1,4-hydroxycarbonyls are an important first generation product in SOA formation from alkanes, as reported by Reisen et al.[49].

Similarly, the formation of alkoxyhydroperoxy aldehyde from reactions of cyclic alkenes and O_3 was reported[53]. These compounds can isomerize via intramolecular reaction between the hydroperoxyl and carbonyl groups to form a cyclic peroxyhemiacetal. Other products such as ketones and lactones are identified from the reaction of cholestane, squalane and octacosane, with OH[48,54]. The octacosanone and octacosanol positional isomers, which are the most prominent first-generation products, were observed during octacosane oxidation. In addition, cholestanones, cholestanals, and cholestanols, are the dominant first-generation functionalization products observed from cholestane oxidation accounting for <70% of the mass of total speciated compounds. Second-generation oxidation products (i.e., fragmentation) and higher-generation products (i.e., functionalization) are much less abundant. For the cyclic compounds, tertiary-carbon alkoxy radicals may have a role in the distribution of functionalization (via isomerization) and the fragmentation products (via decomposition)[48,54].

In the photooxidation of dodecane under high-NO_x, $RO_2 + NO$ gas-phase chemistry forms RO species, which decompose to aldehydes or isomerize to alcohols[31]. Alcohols, hemiacetals, nitrate-bearing hemiacetals, and acid anhydrides are the major SOA products with minor components of dihydrofurans, furans and ketones. Whereas cyclododecane SOA produced under high-NO_x conditions is primarily composed of ethers, esters, hydroxycarbonyls, alcohols, and nitrates. Similarly, hexylcyclohexane SOA produced under similar conditions contains an abundance of oligomeric compounds: hydroxycarbonyl dimers, hemiacetals, and esters[31]. For dodecane oxidation, a distinct feature is the formation of an ester or ether group formed from the dihydrofuran oxidation by either OH or O_3[55]. The formation of tetrahydrofuran and carbonyl ester solely occur via the OH oxidation channel. However, ozonolysis produces an energy-rich primary ozonide, which rapidly decomposes into Criegee intermediates. Similarly, Li et al.[56] also observed the formation of hydroxycarbonyls, hemiacetals, and acid anhydrides, under high-NO_x conditions from the oxidation of long-chain *n*-alkanes

Table 2. Aromatic precursors and reaction products.

Precursors	Experimental conditions	Reaction products	References
Toluene	Outdoor smog chamber, sunlight-irradiated hydrocarbon−NO_x mixtures	3-Methyl-2,5-furandione, dihydro-2,5-furandione and 2,5-furandione, 2-methyl-4-nitrophenol, 3-methyl-4-nitrophenol and benzoic acid	Forstner et al.[68]
	OH radical, chamber, high NO_x	Methylnitrophenols, methyldinitrophenols, methylbenzoquinones, methylcyclohexenetriones, 4-oxo-2-butenoic acid, oxo-C5-alkenoic acids, hydroxy-C3-diones, hydroxyoxo-C5- alkenals, hydroxyoxo-C6-alkenals, and hydroxydioxo-C7- alkenals	Jang and Kamens[70]
	OH radical, smog chamber	Glyoxal, and α-dicarbonyls	Volkamer et al.[72]
	Cl, smog chamber	Benzaldehyde and benzyl alcohol	Wang et al.[92]
	OH radical, chamber, NO_x	Hemiacetal and PHA oligomers and low-molecular-weight dicarboxylic acids	Sato et al.[71]
	OH radical, chamber	1,2-Dicarbonyls glyoxal, methylglyoxal, and biacetyl	Arey et al.[73]
	Flow reactor, OH radical	Bicyclic and ring scission products (e.g. butenedial and methylbutendial), alkyl carbonyls, dienedial and epoxide products	Birdsall and Elrod[62]
	Chamber, OH	Carbonyl (ketone or aldehyde) and acid (carbonyl acid and hydroxycarbonyl)	Li et al.[79]
	Chamber, NO_x	2-Methyl-4-nitrophenol and methyl nitro-catechol	Pereira et al.[78]
	Cl, chamber, NO_x	Benzenetriol, benzoquinone, benzaldehyde, phenols, and benzoic acid	Dhulipala et al.[93]
m-Ethyltoluene	Outdoor smog chamber, sunlight-irradiated hydrocarbon−NO_x mixtures	3-Ethyl-2,5-furandione, 3-methyl-2,5-furandione, 3′-methylacetophenone, 2,5-furandione, and 3-ethylbenzoic acid	Forstner et al.[68]
p-Ethyltoluene	Outdoor smog chamber, sunlight-irradiated hydrocarbon−NO_x mixtures	3-Ethyl-2,5-furandione, 3-methyl-2,5-furandione, 4′-methylacetophenone, *p*-tolualdehyde, and 2,5-furandione	Forstner et al.[68]
Benzene	OH radical, smog chamber	Glyoxal, and α-dicarbonyls	Volkamer et al.[72]
	Flow reactor, OH radical	Bicyclic and ring scission products, alkyl carbonyls, dienedial and epoxide products	Birdsall and Elrod[62]
	Chamber, OH	Ring-opened carboxylic acids and nitrophenols	Sato et al.[77]
	Chamber, OH	Carbonyl (ketone or aldehyde) and acid (carbonyl acid and hydroxycarbonyl)	Li et al.[79]
Ethylbenzene	Outdoor smog chamber, sunlight-irradiated hydrocarbon−NO_x mixtures	3-Methyl-2,5-furandione, *p*-tolualdehyde, 4-methyl-2-nitrophenol, 2,5-hexanedione, dihydro-2,5-furandione, and *p*-toluic acid	Forstner et al.[68]
	Flow reactor, OH radical	Bicyclic and ring scission products, alkyl carbonyls, dienedial and epoxide products	Birdsall and Elrod[62]
Pentamethylbenzene and hexamethylbenzene	Chamber, OH	Carbonyl (ketone or aldehyde) and acid (carbonyl acid and hydroxycarbonyl)	Li et al.[79]
1,2,4-Trimethylbenzene	Outdoor smog chamber, sunlight-irradiated hydrocarbon−NO_x mixtures	4-Methylphthalic acid, 3-methyl-2,5-furandione, 3,4-dimethylbenzoic acid, 3-methyl-2,5-hexanedione, and 2,5-furandione	Forstner et al.[68]
	OH radical, smog chamber	Diacetyl, aldehydes, dimethylphenols, unsaturated dicarbonyls and epoxydicarbonyls	Bethel et al.[69]
	Flow reactor, OH radical	Bicyclic and ring scission products, alkyl carbonyls, dienedial and epoxide products	Birdsall and Elrod[62]
	Chamber, OH	Carbonyl (ketone or aldehyde) and acid (carbonyl acid and hydroxycarbonyl)	Li et al.[79]
1,2,3-Trimethylbenzene	OH radical, smog chamber	Diacetyl, aldehydes, dimethylphenols, unsaturated dicarbonyls and epoxydicarbonyls	Bethel et al.[69]
	Flow reactor, OH radical	Bicyclic and ring scission products, alkyl carbonyls, dienedial and epoxide products	Birdsall and Elrod[62]
1,3,5-Trimethylbenzene	OH radical, chamber, high-/low- NO_x	3,5-Dimethylbenzaldehyde, nitrogenated compounds, furanone and dicarbonyls	Wyche et al.[76]
	Flow reactor, OH radical	Bicyclic and ring scission products, alkyl carbonyls, dienedial and epoxide products	Birdsall and Elrod[62]
	Chamber, OH	Ring-opened carboxylic acids and nitrophenols	Sato et al.[77]
1,2,4,5- Trimethylbenzene	Chamber, OH	Carbonyl (ketone or aldehyde) and acid (carbonyl acid and hydroxycarbonyl)	Li et al.[79]

Table 2 continued

Precursors	Experimental conditions	Reaction products	References
Trimethylbenzenes	OH radical, chamber	1,2-Dicarbonyls glyoxal, methylglyoxal, and biacetyl	Arey et al.[73]
m-Xylene	Outdoor smog chamber, sunlight-irradiated hydrocarbon−NO_x mixtures	3-Methyl-2,5-furandione, *m*-toluic acid, and 2,5-furandione	Forstner et al.[68]
	Flow reactor, OH radical	Methylglyoxal, 4-oxo-2-pentenal and 2-methyl-4-oxo-2-butenal, and dimethylphenols	Zhao et al.[74]
	Flow reactor, OH radical	Bicyclic and ring scission products, alkyl carbonyls, dienedial and epoxide products	Birdsall and Elrod[62]
	NO_3 radical, chamber	Alkylnitrophenols, substituted quinones and HNO_3	Olariu et al.[101]
	Chamber, OH	Carbonyl (ketone or aldehyde) and acid (carbonyl acid and hydroxycarbonyl)	Li et al.[79]
	Chamber, OH	Dicarbonyls, C3-trione, 2,3-butanedione, and 3-methyl-2-oxiranecarbaldehyde	Zhang et al.[80]
p-Xylene	Outdoor smog chamber, sunlight-irradiated hydrocarbon−NO_x mixtures	Acetophenone, 3-methyl-2,5-furandione, 2,5-furandione, dihydro- 5-methyl-2-furanone, benzaldehyde, 3-ethyl-2,5-furandione, and ethyl nitrophenol	Forstner et al.[68]
	OH radical, smog chamber	Diacetyl, aldehydes, dimethylphenols, unsaturated dicarbonyls and epoxydicarbonyls	Bethel et al.[69]
	OH radical, chamber	Unsaturated diketones and unsaturated dialdehydes, and PHA	Song et al.[75]
	Flow reactor, OH radical	Bicyclic and ring scission products, alkyl carbonyls, dienedial and epoxide products	Birdsall and Elrod[62]
	Chamber, OH	Dicarbonyls, C3-trione, 2,3-butanedione, and 3-methyl-2-oxiranecarbaldehyde	Zhang et al.[80]
o-Xylene	OH radical, chamber	Unsaturated diketones and unsaturated dialdehydes, and PHA	Song et al.[75]
	Flow reactor, OH radical	Bicyclic and ring scission products, alkyl carbonyls, dienedial and epoxide products	Birdsall and Elrod[62]
	Chamber, OH	Dicarbonyls, C3-trione, 2,3-butanedione, and 3-methyl-2-oxiranecarbaldehyde	Zhang et al.[80]
Xylene	OH radical, smog chamber	Glyoxal, and α-dicarbonyls	Volkamer et al.[72]
	OH radical, chamber	1,2-Dicarbonyls glyoxal, methylglyoxal, and biacetyl	Arey et al.[73]
1-Methylnaphthalene	Cl, smog chamber	1-Naphthaldehyde and 1-naphthyl alcohol	Wang et al.[92]
2-Methylnaphthalene	Outdoor smog chamber, sulfate aerosols	**OS ($C_6H_4NO_6S^-$, $C_9H_{11}O_5S^-$, $C_{11}H_{13}O_7S^-$, and** $C_{11}H_{11}O_7S^-$**)** and sulfonates	Riva et al.[127]
Naphthalene	OH, UV smog chamber	Naphthalic anhydride, naphthalene-1,8-dicarbaldehyde, naphthaldehyde, oxaacenaphthylene-2-one, and hydroxyl-naphthaldehyde	Riva et al.[212]
	Cl, UV smog chamber	Phthalic anhydride, chloronaphthalene, 1,8-naphthalic anhydride, acenaphthenone, acenaphthenequinone, and chloroacenaphthenone	Riva et al.[91]
	OH radical, chamber, high NO_x	2-Formylcinnamaldehyde, phthaldialdehyde, phthalic anhydride, phthalic acid and hydroxy phthalic acid, benzoic acid, hydroxy benzoic acid, cinnamic acid, dihydroxy cinnamic acid, and **4-nitro-1-naphthol**	Kautzman et al.[85]
	OH radical, chamber, low NO_x	Naphthol, naphthoquinone, epoxyquinone, phthalic acid and hydroxy phthalic acid, benzoic acid, hydroxy benzoic acid, cinnamic acid, and dihydroxy cinnamic acid	
	Outdoor smog chamber, sulfate aerosols	OS (**$C_{10}H_9O_6S^-$**, $C_{10}H_9O_7S^-$, $C_{10}H_{11}O_7S^-$, and $C_{10}H_{10}NO_9S^-$) and sulfonates ($C_6H_5O_4S^-$, and $C_7H_5O_4S^-$)	Riva et al.[127]
Acenaphthylene	OH radical, chamber	Naphthalene-1,8-dicarbaldehyde, 1,8-naphthalic anhydride,10-carbon ring opened dialdehyde, and acenaphthenequinone	Zhou and Wenger[83]
	NO_3 radical, chamber	Oxygenated compounds with C=C bonds, and acenaphthenequinone	Zhou and Wenger[83]
	OH, UV smog chamber	Naphthalic anhydride, naphthalene-1,8-dicarbaldehyde, naphthaldehyde, oxaacenaphthylene-2-one, and hydroxyl-naphthaldehyde	Riva et al.[212]
	Cl, UV smog chamber	Phthalic anhydride, **chloronaphthalene**, 1,8-naphthalic anhydride, acenaphthenone, acenaphthenequinone, and **chloroacenaphthenone**	Riva et al.[91]

Table 2 continued

Precursors	Experimental conditions	Reaction products	References
Acenaphthene	OH radical, chamber	Nitroacenaphthene, 1,8-naphthalic anhydride and 1-acenaphthenone	Zhou and Wenger[84]
	NO_3 radical, chamber	1-Acenaphthenone and nitroacenaphthene	Zhou and Wenger[84]
	Cl, UV smog chamber	Phthalic anhydride, **chloronaphthalene**, 1,8-naphthalic anhydride, acenaphthenone, acenaphthenequinone, and **chloroacenaphthenone**	Riva et al.[91]
Phenol	NO_3 radical, chamber	2-Nitrophenol	Bolzacchini et al.[98]
	NO_3 radical, O_3, chamber	2-Nitrophenol, 4-nitrophenol and *p*-benzoquinone	Bolzacchini et al.[98]
	NO_3 radical, chamber	Nitrophenol, non-aromatic/ring-opening nitro-products, and nitrated diphenyl ether dimers	Mayorga et al.[97]
o-, *m*-and *p*-Cresol	NO_3 radical, chamber	Alkylnitrophenols, substituted quinones and HNO_3	Olariu et al.[101]
4-Methyl catechol	Chamber, NO_x	Methyl nitro-catechol	Pereira et al.[78]
Catechol, 3-methylcatechol, 4-methylcatechol and guaiacol	NO_3 radical, chamber	Nitrophenol, non-aromatic/ring-opening nitro-products, and nitrated diphenyl ether dimers	Mayorga et al.[97]
Catechol	NO_3 radical, chamber, NO_x	4 Nitrocatechol	Finewax et al.[102]
	OH radical, chamber, NO_x	4 Nitrocatechol, and 5-nitro-1,2,3-benzenetriol	
Resorcinol (1,3-benzenediol)	NO_3 radical, chamber, NO_x	Benzenetriol (p), nitrobenzenetriol (p), hydroxymuconic semialdehyde (p), hydroxybenzoquinone (g), and nitroresorcinol (g)	Finewax et al.[103]
	OH radical, chamber, NO_x	Benzenetriol (p), nitrobenzenetriol (p), hydroxybenzoquinone (p), hydroxymuconic semialdehyde (p), benzenetetraol (p) and hydroxybenzoquinone (g)	

*Bold: SOA tracer. *OS* Organosulfates, *p* particle phase, *g* gas phase.

(C_{12}, C_{15} and C_{17}). Recent chamber experiments that examined SOA composition from *n*-alkane (C_{10}-C_{17}) precursors in the presence of NO_x also reported the formation of cyclic hemiacetal, hemiacetal nitrate and hemiacetal dinitrates to be first, second and later generation products[57].

Overall, the hydroxycarbonyl, the most dominant first-generation product from the alkane oxidation (via isomerization of RO), can undergo heterogeneous cyclisation and dehydration to form a substituted dihydrofuran[21,22,33,49–52,55], which is likely to be highly reactive with OH, O_3 and NO_3 due to the presence of a double bond. In addition, tertiary-carbon RO are thought to be key species in the formation of the functionalization and fragmentation products for the cyclic compounds.

Aromatic compounds

Aromatic compounds are generally associated with anthropogenic activities, such as combustion emissions and industrial solvents[10]. Their contribution can reach up to 40% of the total mass of anthropogenic VOC emissions within cities[58]. In addition, the total aromatic emissions (~15.8 Tg y^{-1}) account for 15% of the annual anthropogenic non-methane hydrocarbon (NMHC) global budget[59,60]. Aromatic VOCs can yield a wide variety of secondary oxygenated and nitrated volatile, semi-volatile and non-volatile organic products. Considering the complexity involved in the aromatic VOCs oxidation in the atmosphere, we will discuss the reaction scheme first. This is followed by the discussions about the major oxidation products for different aromatic precursors (mono & poly aromatics).

Formation pathways. Atmospheric oxidation of aromatic hydrocarbons is dominated by reaction with OH, resulting in the formation of a variety of oxidation products via ring-retaining and -opening chemical pathways[58]. Briefly, the OH initiated oxidation of aromatics (≥90%) proceeds via OH-addition to the ring yielding an aromatic-OH-adduct (Ar-OH-adduct), also known as the hydroxycyclohexadienyl radical (and its methylated derivates)[61–63]. An example of the available reaction pathways has been given for the reaction of 1,3,5-trimethylbenzene (1,3,5-TMB) with the OH radical (Fig. 2). Dealkylation and the H-atom abstraction from substituent alkyl groups are minor reaction pathways[62,64,65]. The fate of the Ar-OH-adduct is dominated by reactions with O_2 via reversible/ irreversible pathways. The products of the Ar-OH-adduct + O_2 reactions are phenols (C), epoxides (E), and a bicyclic peroxy radical (G). Formation of oxepins (H) has been observed but not in the case of OH + benzene[66]. The bicyclic peroxy radical ($biRO_2$) is a major product from aromatic oxidation with formation yields of >50% for alkylbenzenes[67]. The reaction of $biRO_2$ is further assumed to yield bicyclic hydroperoxides (K), bicyclic diols (L), and bicyclic ketones (M). The ring opening could potentially lead to the formation of α-dicarbonyls (e.g., glyoxal, methylglyoxal, and dimethyl-glyoxal), unsaturated γ-dicarbonyls (e.g., butenedial, 4-oxo-2-pentenal) and furanones or a combination of these products.

Major reaction products. Outdoor smog chamber photooxidations of toluene, *m*-xylene, *p*-xylene, ethylbenzene, *m*-ethyltoluene, *p*-ethyltoluene, and 1,2,4-TMB have been conducted in the presence of sunlight and hydrocarbon−NO_x mixtures[68]. This study reported that unsaturated anhydrides (furandiones) are the predominant components of aerosol from all the aromatics, while a significant amount of saturated anhydrides was also observed, which could have resulted from the hydrogenation of the furandiones within the aerosol phase. In particular, the more dominant species identified in toluene SOA include furandiones, phenols and benzoic acid where ~40% are linked to ring-retaining products and ~60% are most probably arising from ring-fragmentation pathways. In the case of *m*-xylene and ethylbenzene, ring-fragmentation products comprise a significant portion of the SOA. The dominant organic products include furandiones

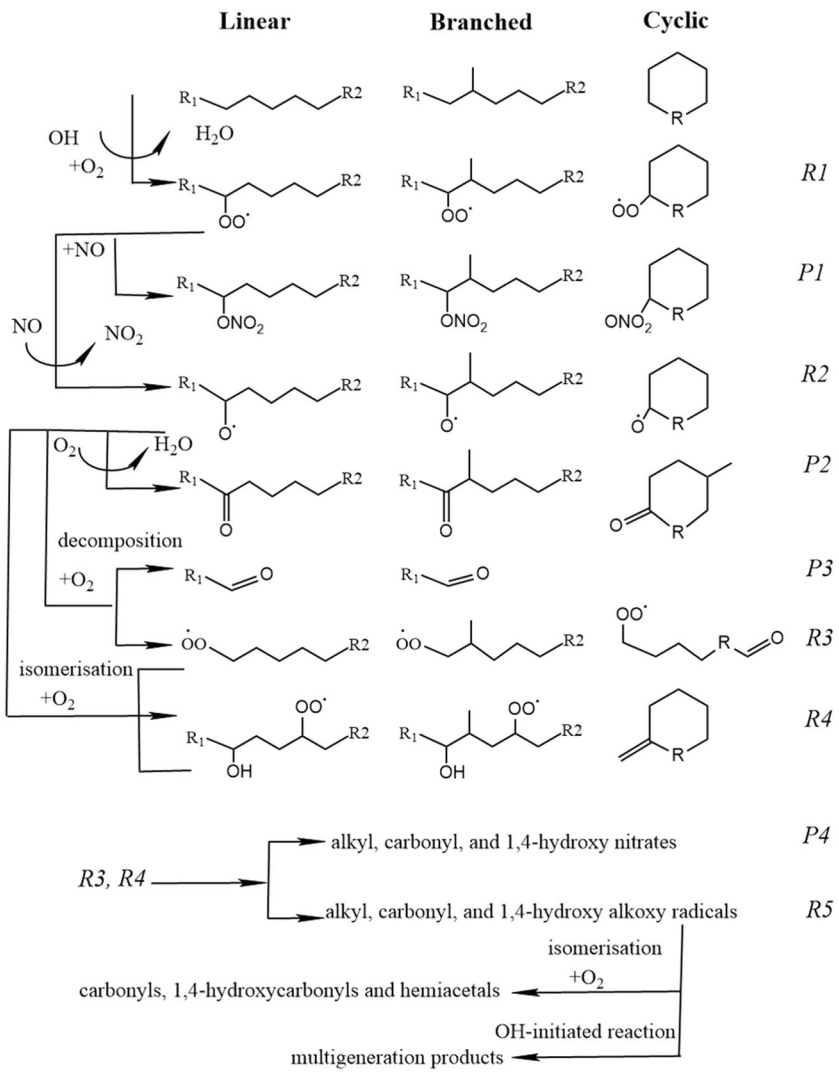

Fig. 1 OH radical-initiated reactions of alkanes in the presence of NO_x. R, R1, and R2 represent alkyl groups (based on the reaction scheme provided by Lim and Ziemann[33]).

and *m*-toluic acid for *m*-xylene with carbonyls, furandiones and phenols for ethylbenzene. In the case of *p*-xylene, SOA was composed of similar products as from *m*-xylene including dicarbonyls and substituted phenols. The ring-retaining and ring-fragmentation pathways were equally as important in 1,2,4-TMB SOA and mainly included benzoic acids, furandiones and carbonyls. Similar products were also observed in *m*- and *p*-ethyltoluene SOA[68]. In addition, ring cleavage products from the gas-phase reactions of the OH radical with *p*-xylene and 1,2,3- and 1,2,4-TMB under varying concentrations of NO_2 included 3-hexene-2,5-dione (32%, 31% percentage yields for *p*-xylene and 1,2,4-TMB oxidation), 2,3-butanedione (52%) from 1,2,3-TMB oxidation[69]. The formation of other ring cleavage products, such as unsaturated dicarbonyls and epoxydicarbonyls, were also observed. Similarly, Jang and Kamens[70] also studied SOA from the photooxidation of toluene. The gas-phase reaction led to substituted aromatics, and non-aromatic ring—retaining and—opening products. The major SOA products included: nitrophenols, quinones, aromatic carbonyls, oxoacids, and unsaturated dicarbonyls. Results also showed that aldehyde products (glyoxal, methylglyoxal, hydroxyacetaldehyde, and some ring-opening products) could further react through heterogeneous processes and contribute to SOA formation. The formation of substituted aromatics and ring cleavage products from the photooxidation of toluene under different NO_x conditions were also reported[71]. The major chemical constituents of the aerosol are hemiacetal, peroxy hemiacetal oligomers and low molecular weight dicarboxylic acids. In addition, peroxy hemiacetal oligomers and dicarboxylic acids were products formed via heterogeneous reactions of second-generation products.

Glyoxal is a major primary product from reactions of benzene, toluene, or xylene (BTX) with OH, indicating that ring-cleavage pathways (bicycloalkyl radical) play a major role in OH-initiated oxidation of monocyclic aromatic VOCs[72]. The formation of primary glyoxal is considered as a marker for the bicycloalkyl radical pathway for benzene oxidation giving a lower limit for the branching ratio for the alkyl-substituted aromatics. In addition, the formation of first-generation products such as α-dicarbonyls (glyoxal and methylglyoxal) and unsaturated 1,4-dicarbonyls via ring scission pathways are also observed[62,68,70]. Similar products were also observed by Birdsall and Elrod[62] and Arey et al.[73] from OH initiated reactions of toluene, xylenes and TMBs. Other products such as dimethylphenols, diunsaturated dicarbonyls and epoxy carbonyls were observed from the photooxidation of *o*- and *m*-xylene in a fast flow reactor at two limiting NO concentrations[74]. Similarly, Song et al.[75] also reported the

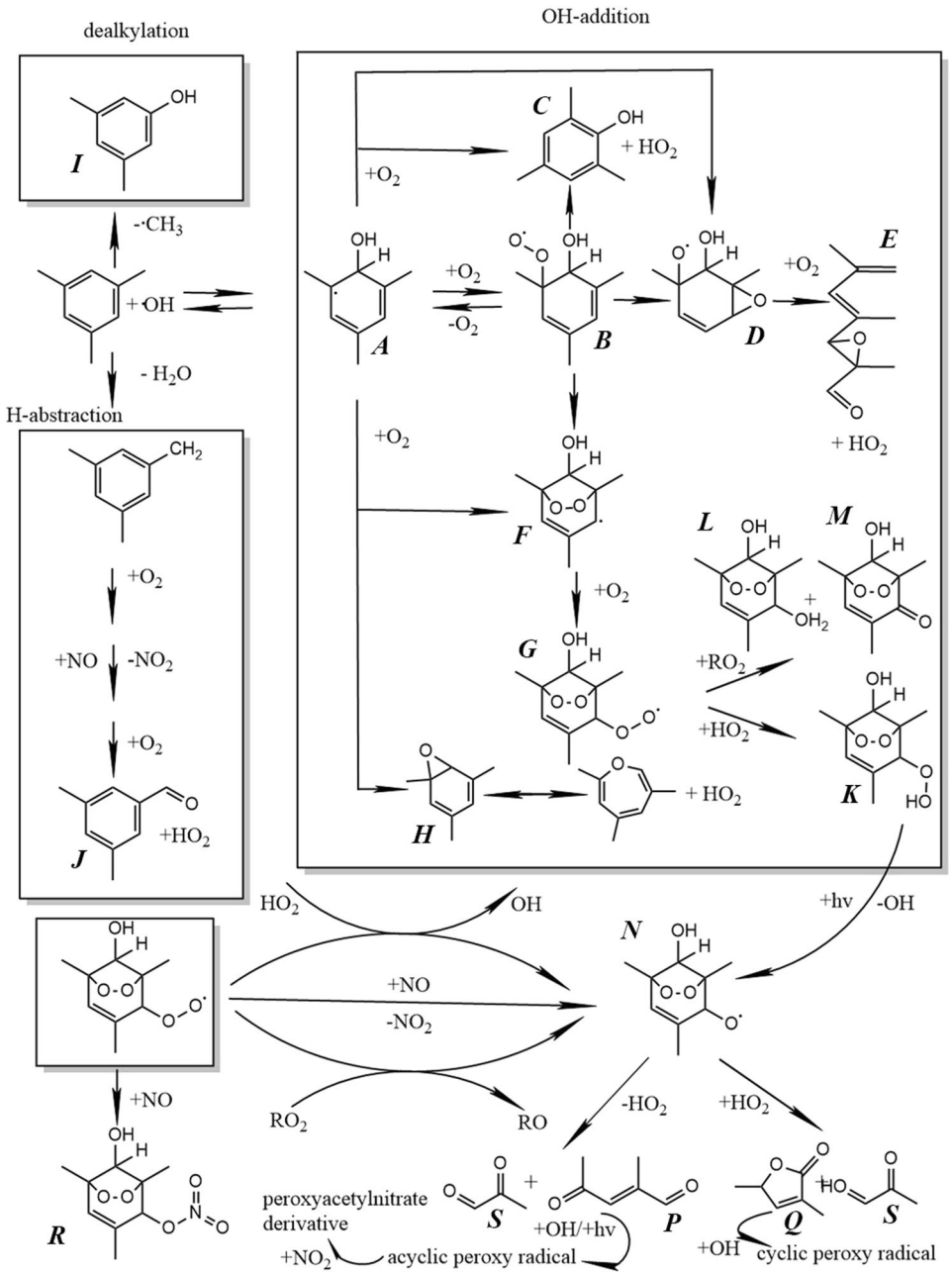

Fig. 2 OH radical-initiated reaction of 1,3,5-trimethylbenzene (1,3,5-TMB). A–S The intermediate products (based on reaction scheme provided by Nehr[240]).

formation of unsaturated diketones and unsaturated aldehydes following the ring-opening pathways, observing dicarbonyls from xylene isomers oxidation.

Oxidation of 1,3,5-TMB was studied under varying NO_x conditions to investigate its potential role in SOA formation[76]. The main reaction products are 3,5-dimethylbenzaldehyde, nitrogenated compounds, furanone and dicarbonyls including low molecular weight organic acids. Methylglyoxal, 3,5-dimethyl-5(2H)-2-furanone, 3-methyl-furan-2,5-dione (methyl maleic anhydride) and the dicarbonyl 2-methyl-4-oxo-2-pentenal, are the first oxidation products formed via the RO and the bicyclic nitrate under high-NO_x. It was proposed that methylglyoxal, the O_2-bridged ketone and the m/z 113 isobaric furanone and dicarbonyl ring-opening products could act as markers to 'represent' SOA formation.

The NO-dependency of the products formed from the OH oxidation of aromatic compounds was also studied[62]. For all aromatic species, the bicyclic peroxy radical and bicyclic peroxide products were uniquely observed. As shown in Fig. 3, the bicyclic species are major products under NO-free conditions with yields ranging from 10 to 30%. It also shows that NO plays a role in the partitioning of the observed products between bicyclic and ring scission products (such as butenedial and methylbutendial for toluene specifically). The presence of NO leads to a higher proportion of ring scission products for each aromatic. The dienedial and epoxide products are observed as minor species in all systems, but not in the case of benzene. For the alkyl carbonyl products, this pathway is much more important for ethylbenzene than for the other alkylated aromatics, which is most likely due to the increased hydrogen abstraction pathway reactivity of the methylene group in ethylbenzene. Similarly, Sato et al.[77] reported the composition of SOA to be abundant with carboxylic acids or hydroxycarbonyls from benzene and 1,3,5-TMB oxidation. The

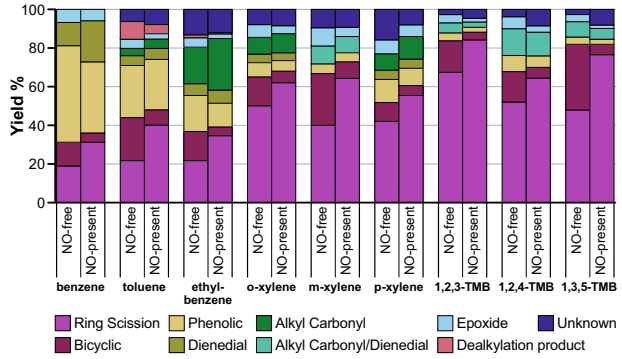

Fig. 3 Summary of products formed from the OH oxidation of aromatic compounds. Yields are also reported for NO-free and NO-present conditions for each compound (taken from Birdsall and Elrod[62]).

carboxylic acids from benzene oxidation contain an aldehyde or carboxyl group while the carboxylic acids from 1,3,5-TMB oxidation consist of a ketone and carboxyl group at each end.

Products from toluene photooxidation under low to modest NO conditions contained 2-methyl-4-nitrophenol, a second-generation product, and methyl nitrocatechol, a third-generation product[78]. In the same study, Pereira et al.[78] also investigated SOA composition formed during the photooxidation of 4-methylcatechol, which did not yield nitrophenols in the aerosol phase; only one nitrophenol (4-methyl-5-nitrocatechol) was observed.

SOA components from the photooxidation of monocyclic aromatics were also investigated by Li et al.[79] and observed the formation of both carbonyls (ketone or aldehyde) and acids (carbonyl acid and hydroxycarbonyl) as seen previously[62,68,70,72,76]. Results also reported that oligomerisation is expected to be an important pathway for SOA formation from monocyclic aromatics. In addition, benzene and toluene were considered as the most important monocyclic aromatic precursors to SOA formation due to their high SOA yields. In addition, SOA products formed during *o*-, *m*-, and *p*-xylene photooxidation were compared by Zhang et al.[80]. This study found that the alkyl substitute position in xylene significantly affects SOA formation, and the effects of NO on the products formed during SOA growth were different for the three xylene isomers. Dicarbonyls, TBM (C_3-trione + 2,3-butanedione + 3-methyl-2-oxiranecarbaldehyde), and highly oxidized species (HOS) were determined to be the predominant SOA components arising from xylene photooxidation[80]. High NO levels were noted to inhibit the formation of C3-trione and 2,3-butanedione in the SOA from *m*- and o-xylene, whereas the formation of 3-methyl-2-oxiranecarbaldehyde during *p*-xylene photooxidation was significantly promoted.

Overall, the major photooxidation products from aromatics (mainly BTX) are glyoxal, methylglyoxal, unsaturated dicarbonyls and furanones via ring-opening pathways, and aromatic aldehydes/acids and phenols via ring-retaining pathways. The hydroxycyclohexadienyl radical, an aromatic-OH adduct, is the main primary product of the reaction of the aromatic ring with OH.

Another important class of compounds is polycyclic aromatic hydrocarbons (PAHs). Those with <4 rings mainly exist in the gas phase and can undergo gas-phase oxidation processes to produce oxygenated and nitro compounds that contribute to SOA formation[81–84]. PAHs can be a potential contributor to the SOA budget, especially in urban areas[81,82]. The OH-initiated photooxidation of naphthalene was examined[85], showing ring-opening products (e.g., 2-formylcinnamaldehyde, phthaldialdehyde, and phthalic anhydride) are the primary gas-phase products under high-NO_x conditions via the $RO_2 + NO$ pathway or a bicyclic peroxy mechanism. The low-NO_x chemistry includes the formation of ring-retaining compounds (e.g., naphthol, naphthoquinone, and epoxyquinone) via the $RO_2 + HO_2$ pathway[85]. Results also suggested that acidic compounds and organic peroxides account for a majority of identified high- and low-NO_x SOA. Organic peroxides are found to contribute ~28 and 26% of the total high-NO_x SOA and low-NO_x SOA mass, respectively. In addition, the study also proposed the use of 4-nitro-1-naphthol as a valid ambient organic tracer for naphthalene high-NO_x SOA.

Simulation chamber experiments studying gas-phase oxidation of acenaphthylene with OH showed the major products were naphthalene-1,8-dicarbaldehyde, 1,8-naphthalic anhydride, and a 10-carbon ring opened dialdehyde[83]. Acenaphthenequinone, a compound known to promote the formation of reactive oxygen species at the cellular level, was also identified as a product of oxidation with OH and NO_3. Ring-retaining and -opening products were also identified from the oxidation of acenaphthene, although nitroacenaphthene, and 1,8-naphthalic anhydride were more abundant in the aerosol phase[84]. In particular, hydrogen abstraction from the cyclopenta-fused ring is reported to be an important reaction pathway for the formation of 1-acenaphthenone and naphthalene-1,8-dicarbaldehyde[84]. Studies of photochemical aging of SOA produced by the gas-phase oxidation of naphthalene by OH and acenaphthylene by O_3 reported naphthaldehyde, oxaacenaphthylene-2-one, and hydroxyl-naphthaldehyde as major SOA products[86].

Role of chlorine (Cl) and nitrate (NO_3) radical initiated oxidation

The above discussion illustrates that OH is central to oxidative processing of anthropogenic VOCs in the troposphere. However, the significance of Cl reactions in the Arctic lower troposphere, marine boundary layer and coastal regions has become apparent[87–89]. The rate constants of reactions of VOCs with Cl are a factor of ~10^2 higher than those with OH[90], implying that even when tropospheric Cl concentrations are relatively low, reactions of VOCs with Cl can be competitive with or even exceed those of OH with VOCs. Similarly, volatile phenolic derivatives are most likely to be emitted from biomass burning and are also produced from the photooxidation of aromatic VOCs. These phenol derivatives can undergo rapid reactions with NO_3 at night and represent a significant source of SOA and brown carbon (BrC) in the atmosphere. Therefore, rapid atmospheric removal is expected upon reactions with OH during the day and NO_3 during the night, suggesting a key role of the NO_3 radical in VOCs oxidation. Details on Cl and NO_3 initiated oxidation of VOCs including their reaction pathway and the major reaction products are discussed here.

Cl radical-initiated oxidation. In the atmosphere, Cl atom-initiated oxidation is possible either via Cl addition to the aromatic ring or H atom abstraction from the ring[91]. Oxidation products from the reaction of Cl atoms with aromatic hydrocarbons include benzaldehyde and benzyl alcohol (95% of total products) from toluene and 1-naphthaldehyde and 1-naphthyl alcohol (48% of total products) from 1-methylnaphthalene (1-MN)[92]. The benzyl peroxy radicals undergo self-reaction to form benzaldehyde and benzyl alcohol in the molecular channel and benzaldehyde via the radical channel.

These products confirm that the hydrogen abstraction reaction is the dominant pathway for oxidation of alkylbenzenes and alkylnaphthalenes, unlike the OH radical reactions, where OH radical addition to the aromatic ring dominates.

Experiments investigating Cl atom-initiated oxidation of naphthalene, acenaphthylene, and acenaphthene show phthalic anhydride and chloronaphthalene as the major products, indicating that both reaction pathways, H atom abstraction and Cl addition are important[91], contrary to the findings reported by Wang et al.[92]. As an example, the proposed mechanism for the Cl atom initiated oxidation of naphthalene is given in Fig. 4. The

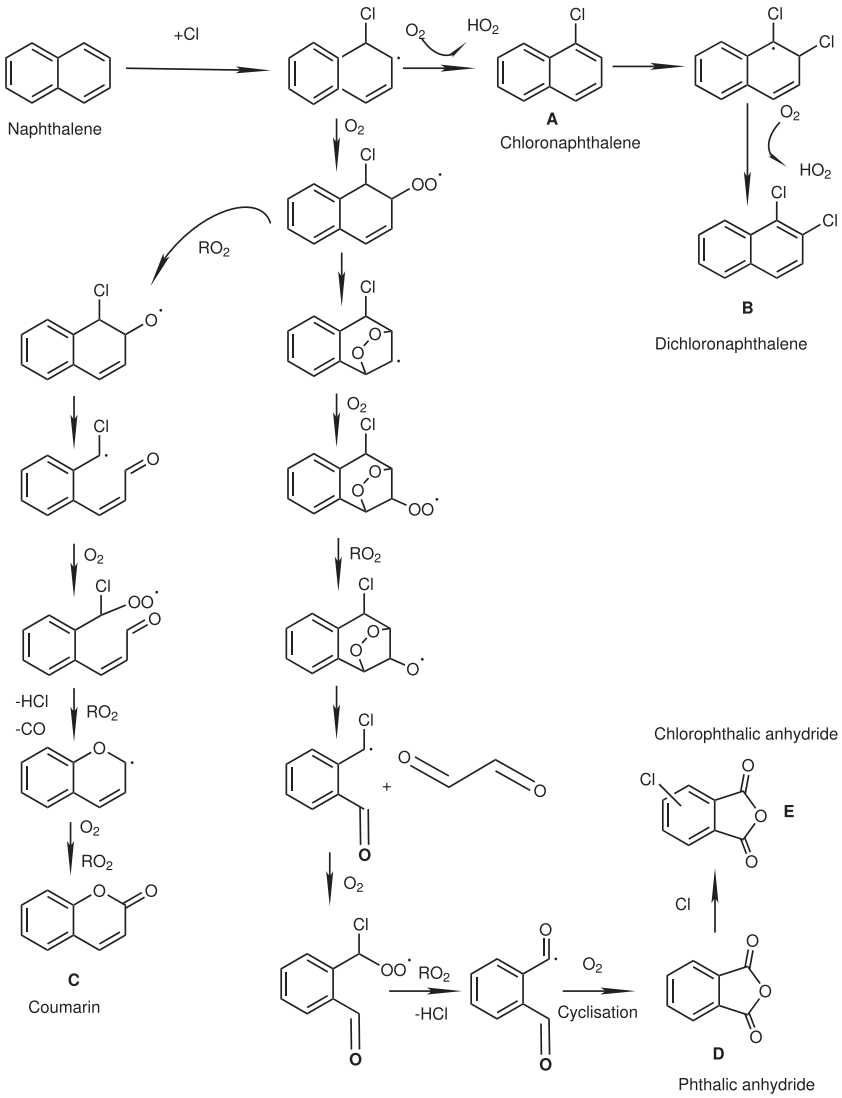

Fig. 4 Formation pathways for the Cl atom-initiated oxidation of naphthalene. A–E represent the products observed in both gas and particulate phase (based on the reaction scheme provided by Riva et al.[91]).

Cl-naphthalene reaction could result in the formation of an RO_2, chlorinated radical, chlorinated oxy radical and acyl radical, where the acyl radical can react with O_2 and then undergo cyclisation to form phthalic anhydride. Acenaphthenone is the main product observed from the reaction of Cl with acenaphthene, while 1,8-naphthalic anhydride, acenaphthenone, acenaphthenequinone, and chloroacenaphthenone were identified as products of acenaphthylene oxidation. The identified oxidation products such as chloronaphthalene and chloroacenaphthenone can be used as potential markers for the Cl atom-initiated oxidation of PAHs.

SOA formation from Cl-initiated oxidation of toluene under different conditions has also been investigated[93]. The difference between high and low NO_x experiments specific to chlorine-initiated chemistry is the formation of $ClNO_2$ in the high NO_x environment, which can result in decreased concentrations of Cl at the beginning of the experiment and also a sustained source of Cl throughout the rest of the experiment. In contrast, in low NO_x experiments most Cl forms HCl, which is relatively stable to photolysis and does not result in significant recycling of Cl. The investigation also showed that bulk organic composition was different for SOA from Cl-dominated reactions compared to OH-dominated reactions, including highly oxidised SOA formed through Cl-initiated reactions. The identified reaction products included benzenetriol, benzoquinone, benzaldehyde, phenols, and benzoic acid.

The formation of organic chlorine upon reaction with alkanes occurs through the heterogeneous production of dihydrofuran via 1,4-hydroxycarbonyl uptake, acid-catalysed isomerization, and dehydration reactions (Fig. 5)[22,33]. Wang and Hildebrandt Ruiz[94] reported the gas-phase alkane—Cl oxidation products formed under high-NO_x conditions were dominated by organonitrates. Organochloride formation is found to be minimal under humid conditions, where dihydrofuran formation is inhibited[95]. The dominant gas-phase organic chlorine compounds were: $C_2H_3ClO_2$ and $C_2H_2Cl_2O_2$. In another study, the Cl-initiated photo-oxidation reactions of n-alkanes: $C_{10} \sim C_{14}$, were also investigated and the formation of carbonyls without any chlorinated products was reported[96], contrary to the results observed by Wang and Hildebrandt Ruiz[94] Decanal and decyl alcohol were the dominant gas phase products of the reaction for n-C_{10} alkane with Cl atom via H-atom abstraction, including two types of reaction with site-internal H-atoms (methylene H atom) and terminal H-atoms (methyl H atom). The oxygenated products continued to react with Cl atoms and then decomposed to form short-chain oxygenated products. In addition, some oxygenated compounds retained the carbon chain after abstracting the methyl H atom and were formed by subsequent reactions with O_2. Similarly,

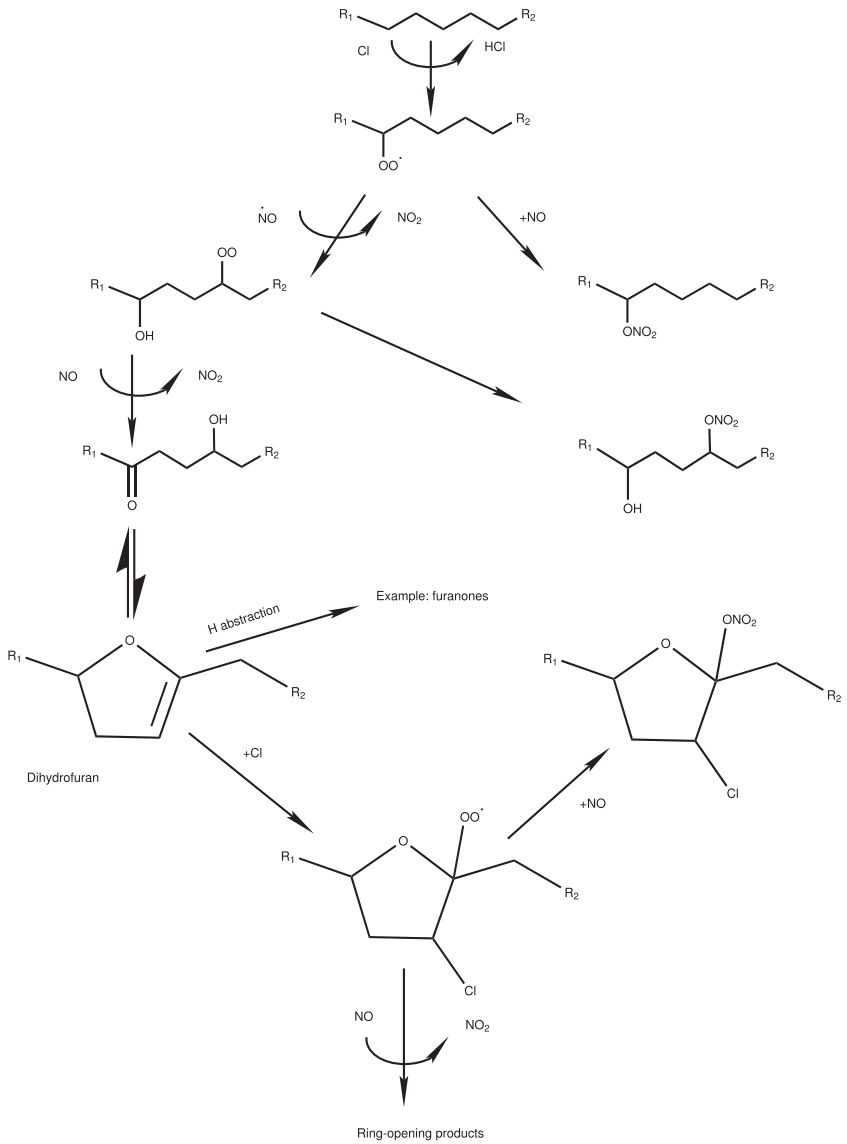

Fig. 5 Formation pathway for the reaction of alkanes with Cl atoms to form chlorinated organics. R1 and R2 represent alkyl groups (based on the reaction scheme provided by Wang and Hildebrandt Ruiz[94]).

$C_{11\sim14}$ n-alkanes also react with Cl atoms by an H-atom abstraction channel; however, they react further with Cl to decompose into small molecule products without retaining the main chain compounds. The reaction of $C_{11\sim14}$ *n*-alkanes with Cl atoms and O_2 led to the initial formation of RO, and further RO arose from three reaction pathways: reaction with O_2 to form carbonyls and continued reaction with the Cl atoms; an intramolecular hydrogen transfer reaction to form alkyl radicals; and decomposition reactions. These reaction pathways could finally form stable compounds with multifunctional aldehydes and ketones as products.

NO3 radical-initiated oxidation. The most common gas-phase reaction scheme for the oxidation of phenolic VOCs is the reaction with NO_3, which leads to the addition of at least one nitro group ($-NO_2$) to the phenolic backbone. The main products from the NO_3 oxidation of phenolic VOCs include the nitro- and dinitro-phenols as well as a variety of their dimer products, which likely undergo gas-particle partitioning (GPP)[97,98]. An example of the reaction pathways is given for the oxidation of phenol with the NO_3 radical in Fig. 6.

The reaction pathway outlined in Fig. 6 has the capability to form a wide variety of dimers upon $NO_3 \cdot$ oxidation with up to three nitrogen atoms per dimer molecule. Many of the dimers in the systems are formed in the gas phase via phenoxy radical pathways, followed by GPP. This is supported as phenol and catechol are present in the dimers; they are unlikely to be present in the particle phase in substantial amounts to participate in condensed phase dimerisation. Similar gas-phase phenoxy radical chemistry has also been proposed previously[99,100].

The reaction of phenol with NO_3 was found to yield 2-nitrophenol as the main nitration product and was independent of the concentration of NO_2[98]. In addition, in the presence of O_3 the formation of 4-nitrophenol and p-benzoquinone was observed. The products formed from the NO_3 radical-initiated oxidation of *o*-, *m*-, and *p*-cresol with high yield were alkylnitrophenols, substituted quinones and HNO_3[101]. The formation of 4-nitrocatechol from the reaction of NO_3/OH with catechol in the presence of NO_x comprises a major component of SOA formed[102]. In addition, the formation of 5-nitro-1,2,3-benzenetriol was also observed from the OH reaction. It was postulated that the formation of 4-nitrocatechol is the result of phenolic hydrogen abstraction by OH or NO_3 to form a β-hydroxyphenoxy/o-semiquinone radical, which then goes on to react with NO_2 to form the final product[102].

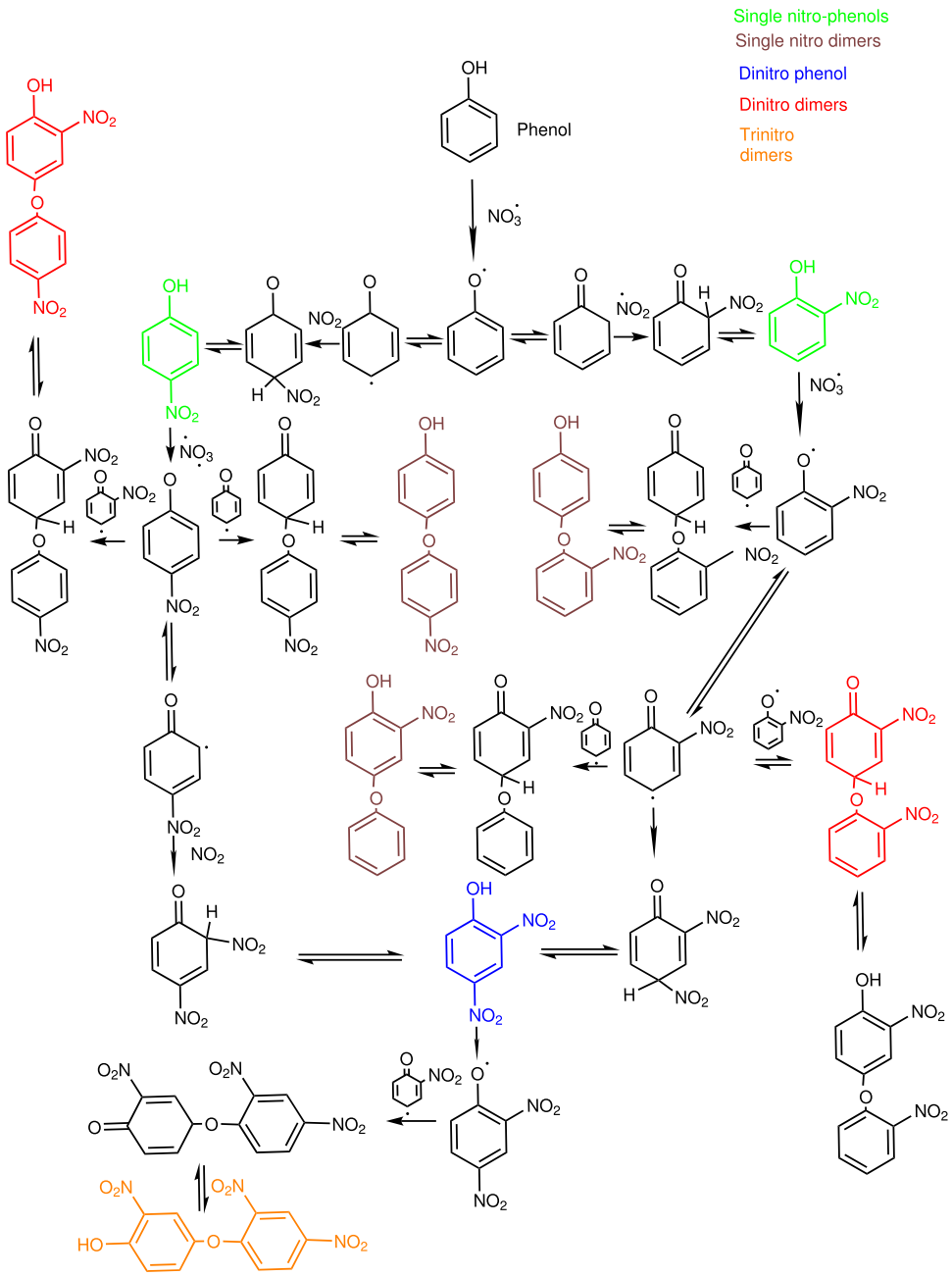

Fig. 6 General mechanism for the NO_3 oxidation of phenol. Green and brown colour represent the products containing single nitro group, blue and red colour represent the products containing two nitro group and orange colour represents the product containing three nitro group (based on reaction scheme provided by Mayorga et al.[97]).

The reaction of resorcinol (1,3-benzenediol) with NO_3 resulted in a lower SOA yield than the OH oxidation[103]. This can be explained by differences in the reaction mechanisms as OH radicals primarily add to the aromatic ring to form a variety of low-volatility products, while reactions with NO_3 radicals occurred solely by abstraction of phenolic hydrogen to produce much more volatile nitroresorcinol and hydroxybenzoquinone products. The major oxidation products identified were benzenetriol, nitrobenzenetriol, and hydroxymuconic semialdehyde in the aerosol phase and hydroxybenzoquinone and nitroresorcinol in the gas phase.

The NO_3 oxidation of five phenolic derivatives (including phenol, catechol, 3-methylcatechol, 4-methylcatechol, and guaiacol) resulted in several nitro-containing products and nitrophenol compounds, including the nitrophenol type of products with additional hydroxyl functional groups, non-aromatic/ring-opening nitro-products, nitrated diphenyl ether dimers and fragmentation products with carbon-containing substituents were investigated[97]. This study indicated that NO_3 oxidation of phenolic VOCs may contribute an important portion of SOA and can lead to a significant portion of light-absorbing BrC in the atmosphere.

Additionally, NO_3 initiated oxidation reactions of PAHs are also particularly important as they can lead to the formation of nitro-PAHs, some of which are known to be mutagenic and carcinogenic[104]. The oxidation products formed from the reaction of NO_3 with acenaphthylene were predominantly composed of oxygenated compounds, including the formation of hydroxylated and nitro-PAHs,

which appears to be very minor[83]. The major gas- and aerosol-phase products from the oxidation of acenaphthene were 1-acenaphthenone and nitroacenaphthene, respectively[84].

Organosulfates—a major SOA constituent

This section is designed to provide a brief introduction to Organosulfates (OS) including their possible formation pathways. In addition, we also focus on the OS compounds identified from the oxidation of anthropogenic precursors such as alkanes and aromatics. During the past decade, OS has gained constant attention with studies reporting a high concentration of OS species in the ambient environment. However, estimates of OS concentrations and their role in atmospheric physicochemical processes are still associated with large uncertainties, suggesting the need for comprehensive research involving field, laboratory, and modelling approaches. The latest review performed by Brüggemann et al.[105] presents extensive information on the formation pathways of OS and their atmospheric relevance, transformations, reactivity, and fate in the atmosphere, and measurement techniques. In addition, the review also highlights a global overview on the OS measurements from different precursors. Therefore, in this section, we will briefly discuss OS and their relevance in the atmosphere avoiding any detailed information which can be easily accessed from the existing review[105].

OS are another important class of compounds and generally considered as potential markers for SOA formation under acidic conditions by aerosol-phase reactions with sulfuric acid[106], formed by oxidation of sulphur dioxide (SO_2). SO_2 is mainly of anthropogenic origin, which suggests the formation of OS can be significant in highly polluted regions around the globe. OS formation possibly occurs through a wider variety of formation mechanisms in the atmosphere, either via heterogeneous or via bulk aerosol-phase reactions, than initially expected. This includes epoxide pathways[107,108], sulfate esterification reactions[109], nucleophilic substitution[109,110], sulfoxy radical reactions[111,112], and heterogeneous reactions of SO_2[113]. The formation of OS via epoxide intermediates is kinetically possible under tropospheric conditions while, OS formation via a direct sulfate esterification pathway may occur rarely. The sulfate esterification needs to be conducted in the absence of water, which is unlikely in the real atmosphere. Despite this, lab studies have reported the formation of OS by direct sulfate esterification[109], but expected to play a less important role in the atmosphere. The OS formation may also occur via nucleophilic substitution of alcohols with sulfuric acid[109,110]. As mentioned, an OS formation pathway is also linked with sulfoxy radical reactions in the aqueous phase via the addition of sulfoxy radicals to double bond molecules[114] or the reaction between a sulfate radical and an alkyl radical[111,112]. The second pathway (radical − radical reactions) is expected to be minor in the presence of dissolved oxygen. In addition, the formation of OS has been also reported through heterogeneous reactions where gas-phase SO_2 reacts with unsaturated hydrocarbons in the absence of gas-phase oxidant like OH or O_3[113].

Several studies have already indicated that OS could account for a substantial fraction (up to 30 %) of the organic mass measured in ambient $PM_{2.5}$[115]. Although most of the evidence for OS identification comes from field measurements[115–117], only a few OS precursors have been characterised through laboratory studies. In most of the laboratory studies, OS has been identified in the presence of acidified sulfate seed aerosol from OH, NO_3 or O_3 oxidation of biogenic VOCs (BVOCs), including isoprene[106,118], 2-methyl-3-buten-2-ol (MBO)[119,120], unsaturated aldehydes[121–123], monoterpenes[109,115] and sesquiterpenes[111,124–126]. Only a few laboratory studies have reported OS formation from anthropogenic precursors[127,128]. However, Ma et al.[129]observed that aromatic OS could account for two-thirds of the OS mass identified in Shanghai. In addition, the formation of aliphatic OS was also reported in the ambient samples from other urban locations[116,117], suggesting that gas-phase oxidation of long-chain or cyclic alkanes could be an important source of OS[116].

The formation of OS from the photooxidation of PAHs (naphthalene and 2-MN) was investigated in the presence of non-acidified and acidified sulfate seed aerosol[127]. Most of the OS compounds identified from the smog chamber experiments were also reported in the samples collected at Lahore, Pakistan, and Pasadena, USA, indicating that PAH photooxidation in the presence of sulfate aerosols can be a source of anthropogenic OS compounds. Results also suggest that some of the identified OS such as $C_{10}H_9O_6S^-$ (m/z 257.0139) from naphthalene photooxidation, and $C_6H_4NO_6S^-$ (m/z 217.9751), $C_9H_{11}O_5S^-$ (231.0333), and $C_{11}H_{13}O_7S^-$ (289.0330) from 2-MN photooxidation can be used as a new PAH SOA tracer[127]. Similarly, the same outdoor smog chamber was used to study the OS formation from alkanes (dodecane, cyclodecane and decalin) photooxidation[128]. Most of the OS identified could be explained by reactive uptake of epoxides onto sulfate aerosol and/or heterogeneous reactions of hydroperoxides. However, OS formation via acid catalysed reactive uptake of epoxides has been observed only for cyclic alkanes. In addition, identified OS such as $C_7H_{15}O_4S^-$(m/z 195), $C_{10}H_{17}O_5S^-$(m/z 249), $C_9H_{19}O_6S-$(m/z 255), $C_{10}H_{19}O_6S^-$(m/z 267), $C_{10}H_{17}O_7S^-$(m/z 281), $C_{10}H_{19}O_8S^-$(m/z 299), $C_{12}H_{19}O_7S^-$(m/z 307), $C_{10}H_{15}O_9S^-$(m/z 311), can be used as tracers for SOA production from the oxidation of alkanes in urban areas. Besides, laboratory evidence for OS formation from anthropogenic precursors is scarce, and thus, more studies are needed to assess the importance and implications of OS for atmospheric composition.

SOA YIELDS

In this section, we summarize SOA yields from the oxidation of alkanes and aromatics based on relevant laboratory studies conducted to date. The data presented here include SOA yields from different precursors under varying atmospheric conditions/parameters. The influence of atmospheric parameters on the SOA yield is discussed later (section 4.2) but also mentioned here when appropriate.

SOA yields: oxidation of alkanes and aromatics from lab studies

Conventionally, SOA formation potential (SOA yield) is defined as the mass ratio of formed SOA and the consumed precursor VOCs (Eq. 10) for a given set of experimental conditions[17].

$$Y(SOA) = \frac{m(SOA)}{\Delta[VOC]} \tag{10}$$

In addition, SOA yield can also be represented as a function of the organic aerosol mass concentration using a semiempirical absorptive GPP model[130,131].

$$Y(SOA) = \Delta M_o \sum_i \frac{\alpha_{iK_{om,i}}}{1 + \Delta M_o} \tag{11}$$

where ΔMo ($\mu g\, m^{-3}$) is the total OA mass concentration, and α_i is the mass-based stoichiometric coefficient for product i that is formed, and $K_{om,i}$ ($m^3\, \mu g^{-1}$) is an equilibrium absorptive partitioning coefficient. Generally, two surrogate species ($i = 2$) have been proven sufficient to parametrize yields.

Details on the measured SOA yields from alkanes and aromatics precursors are given in Tables 3 and 4. Yield estimates are usually based upon quite long reaction times to consume a large proportion of the precursor, but at extended reaction times SOA mass can both increase as more heavily oxidised products are

Table 3. SOA yields from aliphatic precursors.

Alkane-precursors	Experimental conditions	Mass yield	References
Linear alkanes			
$C_{8–15}$ alkanes	Chamber-based high NO_x, OH oxidation	0.05–0.56	Lim and Ziemann[21]
$C_{6–17}$ alkanes	Chamber-based high NO_x, OH oxidation	0–0.877	Lim and Ziemann[33]
C_7 alkanes	OFR, low NO_x, OH oxidation	0.044–0.960	Li et al.[35]
C_8 alkanes	Chamber, high NO_x, Cl, dry/humid	0.16–0.28/0.24	Wang and Hildebrandt Ruiz[94]
C_{10} alkanes	Chamber-based high NO_x, OH oxidation	up to 0.51	Presto et al.[26]
	Chamber-based OH oxidation	0.39, 0.69, 1.1	Lambe et al.[132]
	Chamber-based OH oxidation	0.96–0.25	Hunter et al.[24]
	OFR, low NO_x, OH oxidation	0.044–0.960	Li et al.[35]
	Chamber, high NO_x, Cl, dry/humid	0.45–0.85/0.5	Wang and Hildebrandt Ruiz[94]
C_{12} alkanes	Chamber-based high NO_x, OH oxidation	up to 0.51	Presto et al.[26]
	Chamber-based high NO_x, OH oxidation	0.10	Tkacik et al.[27]
	Chamber-based high NO_x, OH oxidation	0.23–0.62	Loza et al.[23]
	Chamber-based low NO_x, OH oxidation	0.03–0.28	Loza et al.[23]
	Chamber, high NO_x, Cl, dry/humid	1.25–1.65/1.10	Wang and Hildebrandt Ruiz[94]
	OFR, low NO_x OH oxidation	0.044–0.960	Li et al.[35]
C_{15} alkanes	Chamber-based high NO_x, OH oxidation	up to 0.51	Presto et al.[26]
	Chamber-based OH oxidation	0.39, 0.69, 1.1	Lambe et al.[132]
C_{17} alkanes	Chamber-based high NO_x, OH oxidation	up to 0.51	Presto et al.[26]
	Chamber-based OH oxidation	0.39, 0.69, 1.1	Lambe et al.[132]
Tricyclo[5.2.1.$0^{2,6}$]decane	Chamber-based OH oxidation	0.39, 0.69, 1.1	Lambe et al.[132]
Branched			
$C_{6–11}$ branched alkanes	Chamber-based high NO_x, OH oxidation	0.040–0.919	Lim and Ziemann[33]
n-Pentylcyclohexane (C_{11}), 2-methylundecane (C_{12}), 7-methyltridecane (C_{14}), and 2,6,10,14-tetramethylpentadecane (C_{19})	Chamber-based high NO_x, OH oxidation	0.05–.08	Tkacik et al.[27]
2-Methylundecane	Chamber-based high NO_x, OH oxidation	0.05–.08	Tkacik et al.[27]
	Chamber-based high NO_x, OH oxidation	0.11–0.61	Loza et al.[23]
	Chamber-based low NO_x, OH oxidation	0.14–0.65	Loza et al.[23]
Hexylcyclohexane	Chamber-based high NO_x, OH oxidation	0.11–0.61	Loza et al.[23]
	Chamber-based low NO_x, OH oxidation	0.14–0.65	Loza et al.[23]
Cyclic			
$C_{6\text{-}8,10,12,15}$ cyclic alkanes	Chamber-based high NO_x, OH oxidation	0.008–0.613	Lim and Ziemann[33]
C_8 cyclic alkanes	Chamber-based high NO_x, OH oxidation	0.11,0.25	Tkacik et al.[27]
C_{10} cyclic alkanes	Chamber-based high NO_x, OH oxidation	0.11,0.25	Tkacik et al.[27]
	Chamber-based OH oxidation	0.96–1.37	Hunter et al.[24]
	OFR, low NO_x, OH oxidation	1.639–2.121	Li et al.[35]
C_{12} cyclic alkanes	Chamber-based high NO_x, OH oxidation	0.8–1.6	Loza et al.[23]
	Chamber-based low NO_x, OH oxidation	0.22–0.86	Loza et al.[23]
Polycyclic (decalin ($C_{10}H_{18}$), pinane ($C_{10}H_{18}$), tricyclo[5.2.1.$0^{2,6}$]decane ($C_{10}H_{16}$), and adamantane ($C_{10}H_{16}$))	Chamber-based OH oxidation	0.38–1.81	Hunter et al.[24]
Decalin	OFR, low NO_x, OH oxidation	1.532–2.298	Li et al.[35]

formed and decrease due to formation of volatile species in fragmentation reactions of primary oxidation products.

Alkane mass yields. SOA yields for *n*-alkanes ranged from 0.005 for C_8 to 0.53 for C_{15}, with a sharp increase from 0.08 for C_{11} to 0.50 for C_{13}, suggesting this could be linked to an increase in the contribution of first-generation products (hydroxycarbonyls)[21]. Lim and Ziemann[33] also showed a decrease in the SOA yields formed from the oxidation of C_{15}, C_{12}, and C_{10} from 0.63 to 0.35 to 0.15 due to an increase in the amount of volatile reaction products with decreasing carbon number, which subsequently reduces their tendency to form SOA. For branched alkanes, the yields follow the order: C_{12} > 2-methylundecane > 2, 3-dimethyldecane from 0.35 to 0.21 to 0.11. SOA yields were also reported to increase with increasing carbon number (lower volatility) for long-chain *n*-alkanes (C_{10}, C_{12}, C_{15}, and C_{17}), reaching a yield of 0.51 for C_{17} at an organic mass concentration (C_{OA}) of 15.4 μg m^{-3} under high NO_x concentration[26]. However, Lim and Ziemann[33] measured much higher SOA yields than those observed by Presto et al.[26] as their goal was to identify SOA products, thus, the experiments were conducted at much higher C_{OA} (> ~1000 $\mu g\ m^{-3}$).

Tkacik et al.[27] extended the work done by Lim and Ziemann[33] and performed smog chamber experiments with different alkanes, including cyclic, branched, and linear compounds to determine SOA yields with OH radical-initiated reactions under high-NO_x conditions at an atmospheric C_{OA}. SOA yields from cyclic alkanes were comparable to those from linear alkanes with 3–4 carbons larger in size. For alkanes with equivalent carbon numbers, branched alkanes had the lowest SOA yields, ranging between 0.05 and 0.08 at a C_{OA} of 15 μg m^{-3}. The SOA yields from a subset of *n*-alkane precursors (C_{10}, C_{15}, tricyclo[5.2.1.$0^{2,6}$]decane ($C_{10}H_{16}$)) were also investigated and reported maximum SOA yields were 0.39, 0.69, and 1.1[132].

Loza et al.[23] found that the SOA yields were highest from cyclododecane under both NO_x conditions. SOA yields ranged from 0.033 (C_{12}, low-NO_x) to 1.6 (cyclododecane, high-NO_x). Under high-NO_x conditions, SOA yields followed the order 2-methylundecane (0.11–0.38) < C_{12} (0.23–0.62) ~ hexylcyclohexane (0.34–0.61) < cyclododecane (0.8–1.6). Under low-NO_x conditions, SOA yields increased from 2-methylundecane (0.14–0.31) ~ C_{12} (0.03–0.28) < hexylcyclohexane (0.30–0.65) < cyclododecane (0.22–0.86), suggesting a positive influence of cyclization present in the alkane structure. The yields of SOA formed from the reaction of OH with a series of acyclic (C_{10}), monocyclic (cyclodecane ($C_{10}H_{20}$)), polycyclic (decalin ($C_{10}H_{18}$), pinane ($C_{10}H_{18}$), tricyclo[5.2.1.$0^{2,6}$]decane ($C_{10}H_{16}$), and adamantane ($C_{10}H_{16}$)) alkanes, were also examined to better understand the role of multiple cyclic moieties on SOA formation[24]. Results showed that the SOA yield for C_{10}, cyclodecane, decalin, pinane, tricyclo[5.2.1.$0^{2,6}$]decane, adamantane ranged from 0.096–0.254, 0.964–1.37, 1.13–1.38, 0.38–0.396, 0.838–1.81 and 0.99–1.14, respectively. The SOA yields were also investigated from OH oxidation of selected alkanes (C_7, C_{10}, C_{12} and decalin) under low-NO_x condition in an OFR by Li et al.[35] . The SOA yield for C_7, C_{10}, C_{12}, cyclodecane, and decalin ranged from 0.044–0.099, 0.295–0.534, 0.663–0.960, 1.639–2.121, and 1.532–2.298, respectively in the presence or absence of seed aerosols.

Another environmental chamber experiment was carried out to investigate the Cl-initiated oxidation of *n*-alkanes (C_{8-12}) under high NO_x by Wang and Hildebrandt Ruiz[94]. They showed that the observed SOA yields were higher for C_8 (0.16) and C_{12} (1.65) than those resulted from OH-initiated oxidation ($C_8 = 0.04$; $C_{12} = 0.35$). Under humid conditions, the bulk SOA production was found to be suppressed, though the SOA yields observed for Cl-initiated oxidation of C_8 (0.24), C_{10} (0.50), and for C_{12} (1.10) were still much higher than those observed for OH-initiated oxidation.

Aromatic compounds mass yield. Izumi and Fukuyama[133] studied the photochemical aerosol formation from mixtures of aromatic hydrocarbons and NO_x by exposing the gas mixtures to simulated solar radiation in a simulation chamber with the aim of determining the aerosol yields. It was found that yields were greater for toluene, ethylbenzene, and o- and m-ethyltoluene (0.03, 0.031, 0.033 and 0.037, respectively) but lesser for para-substituted toluene derivatives (<0.015). The strong dependency of SOA yields on C_{OA} were observed by Odum et al.[130] who showed that the yield for *m*-xylene and 1, 2, 4-TMB ranged from 0.19–10% and 2.6–9.67%, respectively. Their results also suggest the yield is higher at low temperatures for a given C_{OA}. The SOA yields for 1, 2, 4-TMB derive from experiments conducted at temperatures from 22 to 26 °C. The yield values are like those for both the lower and higher temperature *m*-xylene at C_{OA} below 60 μg m^{-3}. At C_{OA} above 60 μg m^{-3}, the yields for 1, 2, 4-TMB are higher than those for the higher temperature *m*-xylene data and lower than those for the lower temperature *m*-xylene data. Thus, for most atmospherically relevant C_{OA} values (i.e., ≤60 μg m^{-3}), 1, 2, 4-TMB has a similar yield to *m*-xylene.

In addition, an extensive series of sunlight radiated smog chamber experiments were performed with 17 individual aromatic species to determine their SOA yields[131]. The studied VOCs were divided into two distinct classes, namely low- (i.e., ≥ two methyl substituents) and high-yield (i.e., ≤ one methyl or ethyl substituents) aromatics. The SOA yields for low- and high-yield aromatics ranged from 0.019–0.082 and 0.030–0.124, respectively. Similarly, the irradiation experiments conducted in the presence of NO_x reported the largest SOA yield of 1.59 for toluene, followed by 1.09 for *p*-xylene and 0.41 for 1,3,5-TMB[134]. However, Edney et al.[19] observed a lower yield for toluene. The SOA yields were also investigated from the photooxidation of *m*-xylene, toluene, and benzene under two limiting NO_x conditions[25]. Under low-NO_x conditions, the SOA yields for *m*-xylene, toluene, and benzene are broadly constant (0.36, 0.30, and 0.37, respectively), indicating that the SOA formed is effectively nonvolatile under the range of organic mass concentration (>10 μg m^{-3}) studied, whereas under high-NO_x conditions aerosol growth is immediate. Losses of semivolatiles by chemical reaction or to walls lead to lower SOA formation in chambers than in the atmosphere. Considering the slower oxidation rate observed in the photooxidation experiments performed by Odum et al.[130] and Odum et al.[131], it is likely that their SOA yield parameters underestimate SOA formation from aromatic hydrocarbons in the atmosphere. Similarly, the SOA yield from xylene oxidation during *m*-xylene/NO_x experiments showed that at lower NO_x considerably more organic aerosol mass was generated than for those with higher NO_x[135]. The observed SOA yield from xylene oxidation ranged from 0.032–0.141. In a similar experiments, Song et al.[75] investigated SOA formation from the photooxidation of xylene isomers (*m*-, *p*-, and *o*-xylenes), and found that the yield from xylenes ranged from 0.011 to 0.234, strongly depending upon the level of NO_x. A similar SOA yield from the photooxidation of *p*-xylene in the presence of NO_x was also reported by Healy et al.[136]. In addition, Lu et al.[137] investigated another xylene isomer and reported yields with seed (0.05–0.12) and no seed conditions (0.05–0.08), indicating higher yield in the presence of $(NH_4)_2SO_4$ aerosols.

The enhanced SOA yields from 1,3,5-TMB oxidation under low NO_x reported by Wyche et al.[76] indicate a role for oxygen-bridged species and organic acids during aerosol growth. The observed SOA yield ranged from 0.0621–0.0637 and 0.0029–0.0747 under low- and high-NO_x, respectively. Sato et al.[77] showed the SOA yield from benzene to be higher, however, the yield measured (0.025) in one of the experiments was slightly lower than the SOA yield measured by Odum et al.[131] (0.036). SOA formation from the photooxidation of 12 C_8 and C_9 aromatic hydrocarbons under low-NO_x was investigated[138]. Ortho isomers (0.044–0.237) have the highest SOA yield while para isomers (0.024–0.122) have the lowest SOA yield. The lower SOA yields for para isomers are consistent with previous observation by Izumi and Fukuyama[133] and Li et al.[79]. Also, SOA yields of benzene under comparable low-

Table 4. SOA yields from aromatic precursors.

Precursors	Experimental conditions	Mass yield	References
Toluene	Chamber, sunlight-irradiated hydrocarbon $-NO_x$ mixtures	0.015–0.037	Izumi and Fukuyama[133]
	OH radical, chamber, NO_x	1.59	Kleindienst et al.[134]
	Smog chamber, sunlight-irradiated, propene, OH radical	0.019–0.082	Odum et al.[131]
	OH radical, Toluene/propylene/ NO_x /air mixtures	0.021–0.055	Edney et al.[19]
	OH radical, chamber, low- NO_x	0.298–0.308	Ng et al.[25]
	OH radical, chamber, high- NO_x	0.08–0.128	Ng et al.[25]
	OH radical, chamber, low- NO_x, acidic	0.295	Ng et al.[25]
	OH radical, chamber, high- NO_x, acidic	0.167	Ng et al.[25]
	OH radical, chamber, NO_x	0.19–0.38	Chen et al.[139]
	Chamber, OH radical	0.08–0.20	Li et al.[79]
	OFR, OH radical, wet seeds	1.31	Liu et al.[150]
	OFR, OH radical, dry seeds	1.1	Liu et al.[150]
Ethyltoluenes	Smog chamber, sunlight-irradiated, propene, OH radical	0.019–0.082	Odum et al.[131]
o- Ethyl toluene	Chamber, sunlight-irradiated hydrocarbon $-NO_x$ mixtures	0.015–0.037	Izumi and Fukuyama[133]
	OH radical, chamber, low- NO_x	0.141–0.237	Li et al.[138]
m-Ethyltoluene	Chamber, sunlight-irradiated hydrocarbon $-NO_x$ mixtures	0.015–0.037	Izumi and Fukuyama[133]
	OH radical, chamber, low- NO_x	0.020–0.167	Li et al.[138]
p-Ethyltoluene	Chamber, sunlight-irradiated hydrocarbon $-NO_x$ mixtures	0.015–0.037	Izumi and Fukuyama[133]
	OH radical, chamber, low- NO_x	0.039–0.122	Li et al.[138]
Benzene	OH radical, chamber, low- NO_x	0.369	Ng et al.[25]
	OH radical, chamber, high- NO_x	0.281	Ng et al.[25]
	Chamber, OH radical, NO_x	0.018–0.312	Sato et al.[77]
	Photoreactor, OH radical	0.53	Borrás and Tortajada-Genaro[141]
	Chamber, OH radical	0.08–0.35	Li et al.[79]
Ethylbenzene	Chamber, sunlight-irradiated hydrocarbon $-NO_x$ mixtures	0.015–0.037	Izumi and Fukuyama[133]
	Smog chamber, sunlight-irradiated, propene, OH radical	0.019–0.082	Odum et al.[131]
	OH radical, chamber, low- NO_x	0.013–0.167	Li et al.[138]
n-Propylbenzene	Smog chamber, sunlight-irradiated, propene, OH radical	0.019–0.082	Odum et al.[131]
	OH radical, chamber, low- NO_x	0.051–0.054	Li et al.[138]
Pentamethylbenzene	Chamber, OH radical	0.03–0.04	Li et al.[79]
Hexamethylbenzene	Chamber, OH radical	0.02–0.03	Li et al.[79]
Ispropylbenzene	OH radical, chamber, low- NO_x	0.031–0.110	Li et al.[138]
Trimethylbenzenes, dimethylethylbenzenes, tetramethylbenzenes	Smog chamber, sunlight-irradiated, propene, OH radical	0.030–0.124	Odum et al.[131]
1, 2, 4-Trimethylbenzene	OH radical, chamber, propene	0.026–0.0967	Odum et al.[130]
	Chamber, OH radical	0.03–0.07	Li et al.[79]
1,3,5- Trimethylbenzene	OH radical, chamber, NO_x	0.41	Kleindienst et al.[134]
	OH radical, chamber, high- NO_x	0.0029–0.0747	Wyche et al.[76]
	OH radical, chamber, low- NO_x	0.0621–0.0637	Wyche et al.[76]
	Chamber, OH radical, NO_x	0.025–0.156	Sato et al.[77]
	OH radical, chamber, low- NO_x	0.007–0.065	Li et al.[138]
1,2,4,5- Trimethylbenzene	Chamber, OH radical	0.01–0.03	Li et al.[79]
1,2,3- Trimethylbenzene	OH radical, chamber, low- NO_x	0.075–0.119	Li et al.[138]

Table 4 continued

Precursors	Experimental conditions	Mass yield	References
o-Xylene	OH radical, chamber	0.011–0.234	Song et al.[75]
	OH radical, chamber, low- NO_x	0.044–0.091	Li et al.[138]
m-Xylene	OH radical, chamber, propene	0.0019–1.0	Odum et al.[130]
	OH radical, chamber, NO_x	0.032–0.141	Song et al.[135]
	OH radical, chamber, low- NO_x	0.357–0.377	Ng et al.[25]
	OH radical, chamber, high- NO_x	0.035–0.08	Ng et al.[25]
	OH radical, chamber, low- NO_x, acidic	0.404	Ng et al.[25]
	OH radical, chamber, high- NO_x, acidic	0.263	Ng et al.[25]
	OH radical, chamber, NO_x, no seed	0.06–0.08	Lu et al.[137]
	OH radical, chamber, NO_x, seed	0.05–0.12	Lu et al.[137]
	Chamber, OH radical	0.08–0.14	Li et al.[79]
p-Xylene	OH radical, chamber, NO_x	1.09	Kleindienst et al.[134]
	OH radical, chamber	0.011–0.234	Song et al.[75]
	OH radical, chamber, NO_x	0.064–0.13	Healy et al.[136]
	OH radical, chamber, low- NO_x	0.024–0.041	Li et al.[138]
Xylenes	Smog chamber, sunlight-irradiated, propene, OH radical	0.030–0.124	Odum et al.[131]
Naphthalene	OH radical, chamber, low- NO_x	0.58–0.73	Chan et al.[140]
	OH radical, chamber, high- NO_x	0.19–0.39	Chan et al.[140]
	OH radical, chamber, low- NO_x	0.02–0.22	Shakya and Griffin[82]
	Cl, UV smog chamber	0.85–0.98	Riva et al.[91]
1-Methylnaphthalene	OH radical, chamber, low- NO_x	0.58–0.73	Chan et al.[140]
	OH radical, chamber, high- NO_x	0.19–0.39	Chan et al.[140]
	OH radical, chamber, low- NO_x	0.02–0.22	Shakya and Griffin[82]
2-Methylnaphthalene	OH radical, chamber, low- NO_x	0.58–0.73	Chan et al.[140]
	OH radical, chamber, high- NO_x	0.19–0.39	Chan et al.[140]
	OH radical, chamber, low- NO_x	0.02–0.22	Shakya and Griffin[82]
1,2-Dimethylnaphthalene	OH radical, chamber, high- NO_x	0.19–0.39	Chan et al.[140]
Acenaphthylene	OH radical, chamber, low- NO_x	0.02–0.22	Shakya and Griffin[82]
	Cl, UV smog chamber	0.85–0.98	Riva et al.[91]
Acenaphthene	OH radical, chamber, low- NO_x	0.02–0.22	Shakya and Griffin[82]
	Cl, UV smog chamber	0.85–0.98	Riva et al.[91]
Catechol	NO_3 radical, chamber, NO_x	1.50 ± 0.2	Finewax et al.[102]
	OH radical, chamber, NO_x	1.34 ± 0.2	
Resorcinol (1,3-benzenediol)	NO_3 radical, chamber, NO_x	0.09	Finewax et al.[103]
	OH radical, chamber, NO_x	0.86	

NO_x were higher than those in Sato et al.[77]. A similar trend was also observed for SOA yields of toluene[139].

SOA yields were also estimated from PAHs oxidation. SOA formation from photooxidation of naphthalene, 1-MN, 2-MN, and 1,2-dimethylnaphthalene (1,2-DMN) were examined by Chan et al.[140]. This study found SOA yields were 0.19–0.30 for naphthalene, 0.19–0.39 for 1-MN, 0.26–0.45 for 2-MN, and 0.31 for 1,2-DMN under high-NO_x and aerosol mass loadings (10–40 μg m^{-3}). Under low-NO_x, yields were 0.73, 0.68, and 0.58, for naphthalene, 1-MN, and 2-MN, respectively. More ring-retaining products were observed in the gas phase under low-NO_x, resulting in low volatility SOA and constant yields. Their results also showed the SOA yields for naphthalene and alkyl naphthalenes are on the order of 0.25–0.45 under high-NO_x, which are about three times those of light aromatics. Shakya and Griffin[82] determined the aerosol yields for PAHs to be in the range of 0.02–0.22 with 0.20–0.30 uncertainty and in the following order: naphthalene (0.13), 1-MN (0.08), acenaphthylene (0.07), 2-MN (0.06), and acenaphthene (0.06), respectively. High yields for naphthalene may be attributed to larger concentrations of OH and initial ratios of hydrocarbons and NO (HC/NO) compared with the PAH experiments. In addition, the yields reported in their study are within the range of 0.25–0.40 for high NO_x observed by Chan et al.[140]. In another study, the yields (Cl oxidation) were determined to be 0.91, 0.85, and 0.98 for naphthalene, acenaphthylene, and acenaphthene, respectively[91], which is ~3 × higher than from OH oxidation[140].

The yields of SOA formed from reactions of catechol with OH and NO_3 radicals were 1.34 ± 0.2 and 1.50 ± 0.2[102]. These values are exceptionally high, considering that those measured for the photooxidation of simple aromatics ranged from about 0.01 to 0.78 shown above. The SOA yield reported for the OH radical-initiated reaction is much higher than the value of 0.53 reported previously by Borrás and Tortajada-Genaro[141]. In another study, Finewax et al.[103] investigated the SOA formation from resorcinol with OH and NO_3, and SOA yields of 0.86 and 0.09, respectively were reported.

Factors affecting SOA yields

Aerosol yields are dependent on several parameters, such as the concentration of NO_x in the system, the oxidation rate of the precursor, RH, temperature (T) and the type of seed aerosols used. Such factors can influence SOA yields from both anthropogenic and biogenic precursors, although the magnitude of the effect is dependent upon the properties of the individual reaction system. Lower volatile and reactive species are particularly affected by chamber walls losses, which can significantly impact SOA formation experiments as they involve highly reactive oxidants and the production of lower volatility products.

Effects of experimental conditions (i.e., temperature, RH, UV intensity). RH controls the liquid water content of the aerosols and thus the chemical or physical processes that involve water (i.e., reactant, product, or solvent) are affected[14]. However, the number of studies that have systematically investigated the impacts of RH on SOA formation are limited.

Cocker et al.[142] reported the effect of RH on SOA mass yield for the *m*-xylene and 1,3,5-TMB photooxidation in the presence and absence of inorganic (ammonium sulphate, $(NH_4)_2SO_4$) seed aerosol at <2% RH and 50% RH and concluded the impact of RH was not substantial within this range. The effect of RH on SOA formation from the photooxidation of *p*-xylene was also studied at atmospheric pressure and ambient temperature by Healy et al.[136]. They showed an increase in RH results in higher SOA yields and HONO formation, which leads to increased OH concentration. The OH concentration showed a gradual increase with RH and correlated with aerosol yields and RH. In addition, study of SOA formation from toluene and xylenes at different RH also found that increasing liquid water led to increasing SOA formation[143,144].

The formation of SOA from benzene and ethylbenzene in the presence of NO_x at different RH was also investigated[145]. Their results suggested that aqueous-phase reactions and the hydration from glyoxal could be enhanced under high RH conditions, leading to an increase in the formation of SOA from both benzene and ethylbenzene. Hinks et al.[29] studied the effect of RH on the chemical composition of SOA formed from low-NO_x toluene oxidation and showed a significant loss in the amount of oligomers present in the SOA generated at 75% RH compared to that under dry conditions. In addition, their results also confirmed that low-NO_x toluene SOA is more volatile when formed under high-RH conditions[29]. RH-induced oligomer suppression was also reported for Cl-initiated oxidation of *n*-alkanes (C_{8-12}) under high NO_x[94]. SOA yields decreased (0.37 for decane and 0.20 for dodecane) under humid condition (35–67%), similar to the reduction reported in SOA yields for dodecane-OH SOA formation under humid conditions by Fahnestock et al.[31]. Similar results were also observed by Lamkaddam et al.[146] from high-NO_x dodecane SOA formation. Their study reported a reduction in SOA yield by a factor of 2 as conditions went from dry (RH < 1%) to more humid conditions (RH ≥ 5%). The role of water in SOA formation from the irradiation of a toluene-NO_2 system was also investigated by Jia and Xu[147] who reported that the yield of SOA from toluene almost doubled as RH was increased from 5 to 85 %, mainly due to the contribution of O–H-containing products, such as poly alcohols formed from aqueous reactions.

Temperature is another important factor affecting SOA formation due to its effect on both the vapour pressure of the SVOCs and the rate constants of the oxidation processes. Takekawa et al.[20] performed photooxidation experiments to study the temperature dependence of SOA formation from three aromatic hydrocarbons (i.e., toluene, *m*-xylene and 1,2,4-TMB) and one alkane (i.e., n-undecane). Their results showed that a higher SOA yield (~2×) was obtained at 283 K than that at 303 K. In another study the dependence of aerosol mass yield on temperature was investigated in the toluene SOA system[30], which also showed higher SOA yields at lower temperatures (284 K > 305 K) under both low- and high-NO_x, consistent with the previous observation[20]. These results all suggest that many of the oxidation products are semi-volatile and hence partition more extensively into the condensed phase at lower temperatures. An investigation of the temperature dependence of SOA yields for *n*-dodecane ($C_{12}H_{26}$) in the presence of NO_x with and without seed aerosol between 283.0–304.5 K (Fig. 7) showed no strong dependence[32]. This was attributed to a change of rate constants leading to different SOA composition, or non-volatile oxidation products.

UV intensity has also shown a positive effect on SOA yield[26,30]. SOA formed under high- and low-UV intensity showed similar composition as reported by Presto et al.[26]. High SOA yield was expected corresponding to more oxygenated products from increased radical cycling and multigenerational chemistry, but AMS data did not confirm this. In addition, Hildebrandt et al.[30] showed that the toluene SOA formation is sensitive to UV intensity.

Overall, most of the studies showed a positive effect of RH on SOA yields from aromatics through processes which can enhance the SOA formation by aqueous reactions[143–145,147,148]. Unlike RH, temperature has shown a negative effect or little influence on SOA formation due to enhanced partitioning into the condensed phase at lower temperature. In addition, UV intensity also exhibited positive effect on SOA yields.

Effects of molecular structure. The effect of molecular structure/alkyl group position on the measured SOA yield has been investigated[33]. SOA yields from OH radical-initiated reactions of alkanes in the presence of NO_x increase with carbon number due to enhanced formation of non-volatile reaction products. The effect of carbon number of alkanes on SOA composition/yield was also investigated through the oxidation of a range of *n*-alkanes (C_{10}-C_{17})[57]. The relative contribution of first-generation cyclic hemiacetal gradually increased with *n*-alkane size, but the relative contribution of second generation and higher nitrate-containing species (i.e., hemiacetal nitrate and hemiacetal dinitrate) decreased with an increasing alkane size (carbon number). Also, larger decreases for C_{11} were observed compared to C_{17} with increasing RH, indicating that the SOA yield also depends on the size of the parent alkane.

Branched alkanes have lower yields than linear alkanes because of fragmentation and the formation of more volatile products. Cyclic alkanes have higher yields than linear alkanes due to the formation of less volatile ring opened products with an additional aldehyde group. The lower volatility of these products, and their tendency to form oligomers, appears to enhance SOA yields. Presto et al.[26] observed the positive influence of carbon number on SOA yields from *n*-alkanes (C_{10}, C_{12}, C_{15}, and C_{17}) oxidation. SOA yield of branched alkanes also depends on the position of the methyl group on the carbon backbone as suggested by Tkacik et al.[27]. It is possible that a RO adjacent to a branch point predominantly undergoes decomposition leading to fragmentation, and forms products containing fewer carbon atoms that are likely to be too volatile to partition to the particle-phase.

The presence of cyclization in the parent alkane structure has been shown to increase measured SOA yields, whereas the presence of branch points decreases SOA yields, which was more pronounced under high-NO_x than low-NO_x[23]. Higher SOA yields from cyclic and polycyclic precursors have a negligible dependence on the number of rings[24].

For aromatic precursors, alkyl substitution and the *o*-, *m*- and *p*-position affects the SOA yield[131,133]. Odum et al.[131] reported that the single-substituted aromatics might generate a higher ratio of ring-retaining to ring-cleavage products than the multiple-substituted aromatics. Ring-retaining products may have lower vapour pressures than the smaller ring-cleavage products, resulting in higher yields for single-substituted aromatics. In

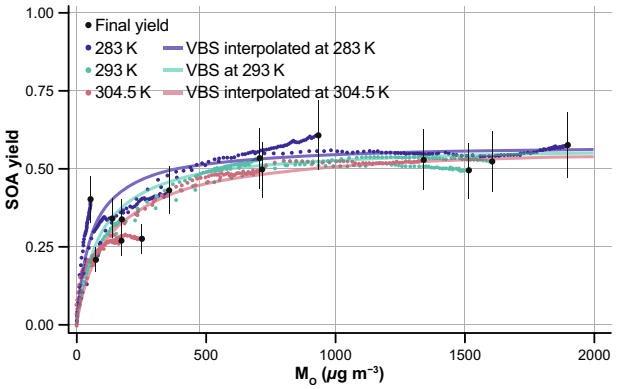

Fig. 7 The *n*-dodecane temperature-dependent SOA yields as a function of the organic aerosol mass. The colours represent the different temperature at which SOA yields were calculated (taken from Lamkaddam et al.[32]).

addition, Li et al.[138] investigated the SOA yield from aromatic oxidation systems and concluded that ortho isomers have the highest SOA yield for similar aerosol concentrations, while para isomers have the lowest SOA yield, showing that SOA yields of aromatic hydrocarbons depends more on the substituent location than substituent length.

Overall, SOA yields from of the oxidation of linear, branched and cyclic alkanes followed the order cyclic > linear > branched[33]. In addition, the position of the methyl group in the branched alkanes and presence of cyclization in the parent alkanes were also found to affect SOA mass yield. SOA yields for aromatic oxidation systems follow the order: ortho > one substituent > meta > three substituent > para, thus showing a significant influence of the alkyl substitute number, substituent location, carbon chain length and branching structure on aromatic hydrocarbon oxidation.

Effects of aerosol seeds. Particle seed characteristics also play an important role in SOA formation. Kleindienst et al.[134] (toluene, *p*-xylene, and 1,3,5-TMB/NO_x), Edney et al.[19] (toluene/ NO_x) and Cocker et al.[142] found that $(NH_4)_2SO_4$ background seed had no significant effect on SOA formation in aromatic photooxidation systems.

However, Kroll et al.[149] and Lu et al.[137] observed that SOA yield was enhanced in the presence of $(NH_4)_2SO_4$ seeds with RH at 4–7 and 56%. The enhanced SOA yield from the photooxidation of aromatic hydrocarbons (e.g., toluene and *n*-xylene) might be attributed to particle phase reactions, which form products with high-molecular weight and low volatility[149]. Lu et al.[137] investigated the effect of inorganic seeds on SOA formation in irradiated *m*-xylene/ NO_x photooxidation systems and proposed that high concentrations of the seed aerosol and thin organic layers are the major factors in particle-phase heterogeneous reactions. The observation that the presence of $(NH_4)_2SO_4$ seed particles impact SOA yields, where $CaSO_4$ and $Ca(NO_3)_2$ particles have no effect, is indicative that the acidic ammonium ion maybe playing a role in the heterogeneous reactions. In another study[25], several *m*-xylene and toluene photooxidation experiments under different NO_x conditions showed that seed acidity has no effect upon SOA yields (Fig. 8).

Kamens et al.[143] showed that experiments with higher initial seed concentrations (and particle phase water) generated more toluene-derived SOA than the lower seed experiments. In addition, Zhou et al.[144] reported that increasing initial seed concentrations resulted in higher SOA yield in the *o*-, *p*-xylene, and toluene SOA system. Liu et al.[150] also investigated the SOA formation from toluene in the absence of NO_x on initially wet or dry $(NH_4)_2SO_4$ seed particles. An increase in OH exposure from 0.47×10^{11} to 5.28×10^{11} molecules cm^{-3} s resulted in a decrease in the ratio of SOA mass yield on wet $(NH_4)_2SO_4$ seeds to that on dry $(NH_4)_2SO_4$ seeds from 1.31 to 1.01. Results showed a relatively higher SOA yield and higher oxidation state of SOA formed with initially wet $(NH_4)_2SO_4$ seeds including SOA composition being dominated by earlier generation products containing carbonyl groups at low OH exposure and by later-generation products containing acidic groups at high OH exposures. In another study, experiments were conducted to assess the effect of seed particles on SOA formation from 2-methoxyphenol (guaiacol) by Liu et al.[151]. With $(NH_4)_2SO_4$ and NaCl seed particles, SOA yield was enhanced by about 23 and 30%, respectively, which further increased to about 30–53% in the presence of SO_2, suggesting that SO_2 and seed particles make a synergistic contribution to SOA formation.

These findings suggest that the presence of seed aerosols may or may not affect the SOA yield, depending upon several factors such as RH, initial seed concentration, acidity etc.

Effects of presence of gaseous pollutants (low/high NO_x conditions). Another important parameter is the level of NO_x; many studies have been conducted to define the influence of NO_x on the SOA yield[25,80,135,140,152–155]. The presence of high NO_x was found to suppress O_3 formation and aerosol formation occurred mainly through reactions with the OH radical in toluene/NO_x photooxidation[152]. Further, the low-NO_x experiments promoted O_3 and NO_3 formation, they can further react with toluene oxidation products, subsequently increasing aerosol formation[141]. In another study, Klotz et al.[153] found that the phenol yield decreased at high NO_x concentrations (>100 ppb) while ring-opening products are favoured during benzene oxidation, suggesting significant differences in aerosol formation between low- and high-NO_x experiments.

Ng et al.[25] showed that the SOA yields from the oxidation of aromatics under low-NO_x is substantially higher than those under high-NO_x. This is likely due to competition between $RO_2 + NO$ (high-NO_x) and $RO_2 + HO_2$ (low-NO_x) reactions, suggesting the importance of RO_2 chemistry in SOA formation from BTX. Under high-NO_x, the RO radical is produced from the reaction of $RO_2 +$ NO which undergoes fragmentation to form higher volatility species, whereas under low-NO_x, the carbon chain is preserved, resulting in higher yields when compared with those observed for high-NO_x. Similar results were also noticed for the toluene and *o*-, *m*- and *p*-xylene isomers oxidation systems[80,154]. Chan et al.[140] also reported the formation of a higher fraction of ring-retaining products under low-NO_x conditions from the oxidation of PAHs. The SOA was composed of semi-volatile products under high-NO_x and nonvolatile under low-NO_x. In a recent study, Yang et al.[155] showed that the SOA yield increases notably with larger NO_x concentrations under low-NO_x conditions during TMB photooxidation, while an opposite trend is observed in high-NO_x experiments. The increase in SOA yield in the low-NO_x regime was attributed to the increase of NO_x-induced OH concentrations; the formation of low-volatility species might be suppressed, thereby leading to a lower SOA yield in high-NO_x conditions.

For linear alkanes with >6 carbon atoms, isomerization of RO is favoured over fragmentation reactions, or reaction with O_2, subsequently resulting in the formation of lower volatility compounds than fragmentation products[22]. Loza et al.[23] observed similar SOA yields under low- and high-NO_x conditions for the larger alkanes (C_{12}), 2-methylundecane, hexylcyclohexane, cyclododecane, suggesting that yields of SOA from alkane oxidation do not display a systematic NO_x dependence. Recently, the roles of NO_x were also investigated by generating individual RO via alkyl nitrite photolysis and measuring their product distributions[156]. Results show that lower-NO/NO_2 ratios promote the formation of secondary OH, peroxyacyl nitrates, and highly oxidized products that result in more SOA production.

The presence of SO_2 has been shown to promote SOA formation in cyclohexane, 2-methothoxyphenol, and TMB

oxidation system[151,155,157]. As discussed before (section 3.4), high SO_2 concentrations may lead to the formation of OS[115–117].

Overall, studies so far have shown that high levels of NO_x may be important factors that lead to lower SOA yields compared to those obtained under low-NO_x conditions for aromatic oxidation systems. However, NO_x dependence for alkane oxidation systems is still not clear. Thus, more studies are needed to investigate the effect of gaseous pollutants in the oxidation system that could deepen the understanding of SOA formation in relatively complex polluted environments.

Effects of OA concentrations, VOC mixtures and TiO_2. The dependence of SOA on OA mass concentration was studied by varying the amounts of VOCs such as *m*-xylene and *p*-xylene[158]. As VOC concentrations increased, the measured OA yield also increased. The OA mass formed in the PAM chamber was directly proportional to the VOC amount during the direct photooxidation of VOCs without seed particles or POA. This is likely due to an increase in the partitioning into the condensed phase which could enhance OA mass concentration[130,159].

SOA yields can also be profoundly affected by oxidation of VOC mixtures. McFiggans et al.[160] demonstrated that highly reactive compounds (e.g., isoprene) can scavenge OH radical, inhibiting their reaction with other VOCs, and the resulting RO_2 can also scavenge highly oxygenated products. These processes can reduce the yield of low-volatility products that may suppress both particle number and mass of SOA.

The effect of photocatalytic materials on SOA formation is still not clear. TiO_2 suppressed SOA formation from the photooxidation of *m*-xylene[161]. Yields of SOA were 0.003–0.04, whereas negligible SOA was formed when TiO_2 was added. This is likely to be due to the decreased concentrations of reactive carbonyl compounds because of TiO_2 addition. The suppression effect was also influenced by the presence of seed particles and NO_x. Reaction mechanisms for the photocatalysis of aromatics should be considered in future under varying experimental conditions.

Overall, results suggest a positive influence of OA mass concentration on SOA formation, while the presence of photocatalytic material and VOC mixtures shows a negative effect.

Effects of chamber walls and OH exposure. SOA yields are highly sensitive to experimental conditions, as well as corrections of the data for chamber wall losses[30,162–165]. Investigations of gas-wall partitioning on SOA yield, that included the oxidation of C_8–C_{16} *n*-alkanes, 1-alkenes, C_8–C_{13} 2-alcohols and 2-ketones in Teflon chambers indicate that losses of OC to the walls can be large for SVOCs and could result in significant underestimation of SOA yields[162]. The possibility of further oxidation or particle-phase oligomer formation is reduced by the loss of gas-phase OC to the walls, thereby directly reducing the SOA yield. Experiments studying the toluene-NO_x oxidation system demonstrated the underestimation of SOA formation by factors up to 4 due to losses of SOA-forming vapours to chamber walls[163]. In addition, gas-phase wall losses for both types of chambers (continuous flow and batch) under similar conditions showed that the continuous flow experiments mitigate some effects of gas-phase wall losses with long (>2 days) experiment run times[165]. These studies show that gas-phase wall losses still affect the absolute SOA yield for both types of chamber and warrant more investigation.

Another important parameter observed during the experiments is OH exposure. Studies have shown a decrease in SOA yield for aromatics/alkanes oxidation systems subsequent to an increase in OH exposure. This is possibly due to further oxidation of gas-phase species and breaking of carbon–carbon bonds or heterogeneous OH oxidation reactions[24,132,166].

Following the above discussion, the observational evidence suggests a significant effect of gas phase wall loss on SOA mass yields, showing a suppression in SOA formation due to loss of SOA

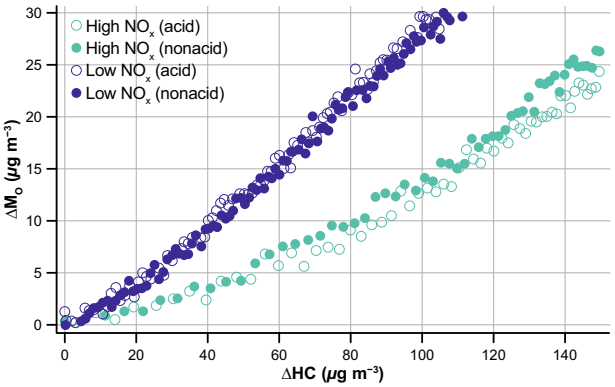

Fig. 8 SOA growth curves for toluene photooxidation in the presence of neutral seed versus acidic seed. Solid and hollow circles represent nonacidic and acidic seed condition (taken from Ng et al.[25]).

-forming vapour. In addition, experimental variables such as OH exposure may have a negative effect on SOA yield.

Perspective on factors affecting SOA yields. As discussed above many parameters affect aerosol yield. Generally, factors like RH, UV intensity, and initial OA mass concentration seem to have a positive influence on SOA formation while temperature, NO_x, OH exposure, the presence of photocatalytic material and VOC mixture shows a negative effect. SOA yield was also found to be highly sensitive to the design of chamber walls, molecular structure of the individual precursor and the presence of seed aerosols. While the role of these parameters is relatively well understood for alkanes and the common mono/poly aromatics-OH oxidation system (using single precursor approach), most of the current challenges and uncertainties, by far, concern their role in real atmospheric conditions where SOA precursors are highly complex mixtures with different volatilities including the presence of other oxidants (e.g., Cl and NO_3). It is thus urgent to assess the effect of these parameters under the real atmospheric conditions by photo-oxidising dilutions from whole major emission sources, such as from vehicular exhaust or biomass burning (and not solely a specific compound from these sources).

SOA ESTIMATION FROM DIFFERENT ANTHROPOGENIC SOURCES

In the previous section, we have discussed alkane and aromatic compound oxidation systems, including their reaction pathways, SOA forming potential (yield), and major reaction products. We briefly present here SOA formation from specific anthropogenic sources such as vehicular exhaust (diesel/gasoline), residential wood burning, cooking etc. Diesel exhaust is an important source of OA in the urban environment, primarily composed of light aromatics, PAHs and long-chain n-alkanes[167–169]. The gas-phase emissions from diesel exhaust are dominated by light aromatics, accounting for 27% of the SOA formed. The SOA contribution from PAHs can reach up to 54% from the oxidation of diesel emissions, representing a potentially large source of urban SOA[140]. Intermediate volatility organic compounds (IVOCs) are found to be a major component of diesel fuel and mainly exist as vapour in the atmosphere[170]. Results also suggest some of the first generation products of IVOC (diesel fuel) oxidation are vapours that can undergo multiple generations of oxidation. IVOCs also contribute similarly to the total SOA budget as PAHs, but higher (~4) than single-ring aromatics[27,171]. The findings also show twice as much SOA formation from diesel emissions after the inclusion of IVOCs as an SOA precursor. Therefore, IVOCs are likely an important source of SOA mass in the atmosphere. In addition,

photooxidation of IVOCs also illustrates that the IVOCs are more likely to form oxygenated OA under high NO_x conditions, contrary to the oxidation of traditional anthropogenic and biogenic SOA precursors for which reduced aerosol formation is observed at high NO_x[172]. For gasoline exhaust, the emissions of PAHs compared to light aromatics are low, hence, their contribution to SOA formation is almost insignificant[173]. In another study, the ageing of gasoline exhaust was performed using a mobile environmental reaction chamber[174]. Results illustrated that a modern gasoline car can lead to the formation of significantly higher SOA than the emitted primary aerosol mass. Du et al.[175] reported higher SOA production from gasoline exhaust, showing a greater contribution of IVOCs and SVOCs to the SOA formation. Similarly, another experimental study with gasoline exhaust also showed the formation of higher amounts of IVOCs and SVOC, which promoted the GPP and SOA formation[176]. It has also been shown that with the increase of aromatic content in gasoline exhaust from 23 to 50%, an enhancement was reported in the SOA yield by a factor of 4.0–6.7[176]. Residential wood combustion can contribute considerably to the atmospheric OA/SOA burden, particularly in regions with cooler climates, and contribute up to ~80% of the total observed SOA[177]. Cooking may also be a potential source of SOA because of the abundant emissions of non-methane organic gases[178]. It has also been shown that the alkenals, which are not traditional SOA precursors accounted for 5 − 34% of the observed SOA[179]. In addition, SOA formation from gas-phase emissions of heated oils were also investigated[178], showing the major SOA precursors were linked to the content of monounsaturated fat and omega-6 fatty acids present in cooking oils. In another study, SOA formation from heated oils also suggested that the major precursor was aldehyde, which accounted for a majority of the oxidation products from cooking emissions[180]. Additionally, there is a growing concern with SOA formation from non-combustion anthropogenic sources (e.g., coatings, adhesives, cleaning agents, printing inks, pesticides, and personal care products), which may contribute a substantial amount of VOCs to the atmosphere and subsequently results in SOA production[181]. However, many of these chemicals are currently not included in the emission inventories and require better quantification.

FACTORS AFFECTING SOA PROPERTIES

The composition and properties (i.e., optical properties, oxidation state, and phase state) of SOA are affected by RH, temperature and SO_2, which has significant implications for regional haze formation and global radiative forcing. Therefore, we discuss in further detail these SOA properties and their implications for air quality and climate.

Optical properties

The optical properties of SOA and their effects on the global radiative balance remains poorly understood. Refractive index (RI) is one of the most important parameters when describing aerosol optical properties as it accounts for other optical factors, such as scattering and extinction efficiencies. RIs measured of seeded aerosols are a little lower than those under non-seeded conditions in low-NO_x environments, but are higher for high-NO_x environments[56]. This was the case most noticeably for dodecane derived SOAs when comparing SOA derived from other long-chain alkanes. Measured RI values generally ranged from 1.33 to 1.57 (i.e., 1.33–1.54 for C_{12}, 1.40–1.57 for C_{15} and 1.41–1.53 for C_{17}-derived SOAs). Long-chain alkanes, a major contributor to IVOC, may contribute largely to the optical properties of SOAs. Multiphase processes can also affect the RI and light-extinction of *m*-xylene-derived SOA. They can significantly enhance the RI due to oligomerisation processes that results in an increase of the light-scattering efficiency and direct radiative forcing by ~20–90%[182].

The optical properties of *m*-xylene-derived SOA are affected by GPP. As organic mass increases and the particles grow, the proportions of SVOCs and IVOCs in the aerosol phase change resulting in a decrease of SOA RI by 0.09 ± 0.02 without seeds and 0.15 ± 0.02 with seeds[183]. Pre-existing seeds could promote condensation and could inhibit the formation of some high-molecular-weight products, like highly oxygenated multifunctional compounds (HOMs), leading to a further decrease of the RI. In addition, the optical properties of SOA particles are related to the total organic mass and molecular composition. Similarly, the optical properties of *n*-dodecane SOA showed that low temperatures could enhance the real part of the RI at wavelengths of 532 and 375 nm due to the formation of large amounts of oligomers[184].

Experiments investigating the effect of different experimental conditions (i.e., dry, dry with SO_2, wet and wet with SO_2) on the composition and optical properties of toluene-derived SOA showed that an increase in the RH enhances both light absorption and the scattering property of the SOA, possibly due to the formation of oligomers through multiphase reactions[185]. The addition of SO_2 resulted in a decrease in the real part of the RI of toluene-derived SOA, probably due to the partitioning of low-oxidation products. The extinction coefficients of toluene-derived SOA with SO_2 increased by ~30% under wet conditions compared to dry conditions.

Carbon oxidation state

The average carbon oxidation state (OS_C) is widely used to describe the degree of oxidation of atmospheric organic species[186]. Briefly, the OS_C is defined as the charge a carbon atom would acquire if it loses all electrons with more electronegative atoms but gains all electrons with less electronegative atoms. Liu et al.[151] reported that SO_2 was found to favour an increase of the OS_C of SOA formed from methoxyphenol oxidation, indicating that a functionalisation reaction is dominant over oligomerisation and leads to the formation of highly oxidised products with relatively low volatility, which consequently result in an increase in OS_C and SOA yields. The formation and ageing of SOA from the photooxidation of toluene and other small aromatics were also studied[187]. Higher exposure to OH resulted in a different OA composition with high OS_C and SOA mass yield and reduced SOA volatility. The OS_C generally increased during photooxidation ranging from 0.16–0.29 for final oxidation products[187]. The cloud condensation nuclei (CCN) potential of aerosols is a function of their hygroscopicity[188]. Hildebrandt Ruiz et al.[187] reported no clear correlation between hygroscopicity and O:C or between hygroscopicity and OS_C in the toluene photooxidation system, contrary to the conventional view that suggests oxidative ageing of aerosol has a positive effect on hygroscopicity[189]. This is possible either due to the presence of surface-active compounds or if the OA is mostly composed of compounds with similar OS_C but different molecular size (e.g., oligomers), as the size of molecules affects their solubility and hence their hygroscopicity. It has also been reported that OS_C is a better indicator of aerosol oxidation than O:C as the latter may have some influence from non-oxidative processes (i.e., hydration and dehydration) while OS_C increases continually with oxidation[186,187]. In another study, experiments investigating the relationship between the oxidation level and hygroscopic properties of SOA particles confirmed that the hygroscopic growth varied linearly with O:C, but the CCN activity mostly followed a nonlinear trend[190].

Physical phase state

The physical phase state (e.g., solid, semisolid or liquid) of SOA particles can significantly affect a number of atmospheric processes, such as gaseous uptake, particle-phase rate of reaction, GPP equilibrium and ageing[191–193]. For example, the diffusion of molecules within the bulk of a viscous particle is comparatively slow and may become the rate-limiting step. The water uptake of highly viscous SOA particles may not occur at low temperatures, which has a significant influence on particle size and scattering properties[193,194]. The RH-dependent viscosities at room temperature of SOA particles produced from toluene photooxidation indicate that the toluene-derived SOA particles are in the liquid phase at RH > 60%[195]. Saukko et al.[192] investigated the phase state of laboratory-generated SOA produced in a flow tube reactor by photooxidation of anthropogenic precursors, naphthalene and *n*-heptadecane. Their measurements of the bounced fraction (BF) suggests that SOA particles are in an amorphous solid or semisolid state at RH < 60%. SOA particles generated from naphthalene showed a decrease in the BF from 0.65 ± 0.1 at RH < 50% to 0.4 ± 0.1 at RH = 64 %, suggesting a decrease in viscosity possibly due to an RH-induced phase change from solid to liquid-like particles. Unlike the naphthalene SOA system, *n*-heptadecane SOA has a low BF indicating liquid-like, less viscous particles at low oxidation levels[181]. In addition, the bounce behaviour of the SOA systems did not always show a correlation with the particle oxidation state[192].

Koop et al.[193] have suggested that the oligomerisation and polymerisation processes should be given greater consideration as they will affect the physical state of organic aerosols beyond the decrease in vapour pressure. Oligomerisation may result in a strong increase in viscosity and the formation of semisolid state aerosols, which has implications for heterogeneous oxidation reactions and the extended atmospheric lifetime of SOA particles[193]. Several other studies have also shown that laboratory-produced SOA particles have an amorphous solid state[191,196–198]. However, recent studies are predominantly based on biogenic precursors suggesting that more studies using anthropogenic precursors are required to better evaluate the change in SOA properties and their impact on the urban environment.

FLOW REACTORS VS SMOG CHAMBERS: EFFECT ON PRECURSOR OXIDATION AND YIELDS

Flow reactors (e.g., PAM) and smog chambers have both been used extensively to study SOA formation for a variety of atmospherically relevant conditions and emission sources. However, large-scale smog chambers age pollutant mixtures over the course of hours to days, whereas flow reactors rapidly age the mixtures in seconds to minutes. They do this by using high oxidant concentrations to achieve higher degrees of oxygenation, which may affect the atmospheric relevance of the generated products. In addition, the ability of flow reactors to simulate slow atmospheric processes, like condensed phase reactions, is also of concern. The chemical composition and yields of the oxidation products formed from the photooxidation of α-pinene and of wood-combustion emissions were generally consistent in both PAM and smog chamber[199]. However, the yields during the PAM experiments for the α-pinene system were slightly lower than those in the smog chamber due to increasing wall losses of gas-phase species as PAM has a higher surface area to volume ratio. Similarly, an intercomparison study of SOA generated from gas-phase precursors in a PAM and several environmental chambers showed a similar SOA composition across all systems, whether low OH concentrations are used over long exposure times (chamber) or high OH concentrations over short exposure times (PAM)[200]. The use of acidic seed particles in the flow reactor increased the yield of SOA by a factor of 3–5, where seed particles are routinely used in the chambers. The study also highlights that both, flow reactors and chambers, are capable of characterising SOA ageing mechanisms representative of ambient conditions. Despite concerns, flow reactors are likely to remain within the study of atmospheric ageing as they produce a high, consistent and reproducible output, are mobile and age aerosols over short timescales, all very convenient attributes for laboratory studies. More intercomparison studies with varying atmospheric conditions for both types of reactors should be considered when evaluating their use within aerosol aging experiments, as commercially available PAM chambers have gained rapid popularity due to their ease of use within field and laboratory experiments.

GAPS IN SOA CONTRIBUTION FROM LAB, FIELD AND MODELLING STUDIES

This section focuses on areas of uncertainty in the understanding of SOA formation from anthropogenic precursors/sources.

Laboratory studies

Most of our knowledge about SOA formation from anthropogenic VOCs (i.e., alkanes, aromatics, alkenes) derives from laboratory studies. These studies are designed to mimic atmospheric conditions using large simulation chambers (also known as smog chambers) or aerosol flow reactors. In general, the potentials of compounds to form SOA are measured using experiments with a single precursor approach[130,201]. However, in reality, SOA precursors occur within packets of air as highly complex mixtures of VOCs and SVOCs with different volatilities[202]. As a result, using a single-species approach for studying SOA formation is not atmospherically representative, especially in the urban environment. Some studies have been performed to avoid issues with the single-species approach by photo-oxidising whole vehicular exhaust or biomass burning emissions[170,177,203–208]. Tiitta et al.[205] and Bruns et al.[177] investigated the SOA formation from fuel-wood-burning emissions and wiregrass fires and found pyrogenic VOCs (e.g., benzene, naphthalene, and toluene) and furans were significant precursors for SOA production. This is in contrast to the findings of Ahern et al.[203], who investigated SOA formation in smoke from the open burning of various biomass fuels representative of canopy and grassland fires and observed significant OA mass enhancement from fuels representing canopy fires containing significant amounts of volatile precursors, such as monoterpenes. Their experiments were conducted using freshly harvested branches of coniferous canopy fuels, a species known as monoterpene emitters[209,210]. Similarly, the OH-initiated ageing of biomass burning emissions was also investigated[204], showing the formed SOA is found to be highly variable and the observed variability may be related to the initial total non-methane organic vapour concentration and OH exposure. In addition, experiments investigating the ageing of emissions from flaming and smouldering-dominated wood fires showed single-ring and polycyclic aromatics are major precursors in flaming emissions, while furans are important SOA precursors in smouldering fires[206]. Results also suggest that the oxidation products from lignin pyrolysis are likely to dominate SOA formation, which does not depend on the combustion or ageing conditions.

Like biomass burning emissions, photooxidation of low volatility organics found in motor vehicle emissions have been investigated[170,207,208]. Experiments with light-duty gasoline vehicle exhaust suggest that the catalyst warm-up is an important factor in controlling SOA precursor emissions[207]. In addition, the majority (<50%) of measured SOA from diesel emissions can be explained by traditional SOA precursors while the rest (~30 %) may originate from the non-methane organic gas emissions[208]. These

observations provide a comprehensive overview on SOA formation considering all VOCs present, which is not possible using the single precursor approach. More studies are needed to get detailed insight on SOA formation mechanisms from key VOC precursors to improve the development of next-generation SOA models and emissions control strategies.

Additionally, laboratory studies have identified linear, branched, and cyclic alkanes with carbon numbers ranging from C_7 to C_{25} as possible SOA precursors while monoaromatics (i.e., benzene, toluene, xylene, TMB) are the most common aromatic precursors as discussed in the previous sections. Cyclic compounds are abundant in diesel exhaust, comprising of ~30% monocyclic and 50% polycyclic alkanes[24,211] Industrial and combustion emissions are also likely to be other sources of polycyclic species. However, SOA formation from polycyclic alkanes has not been explored much, including the effect of multiple, fused rings on SOA formation. PAHs, an important precursor for SOA formation in an urban environment, have not been investigated extensively, except in a few cases[91,92,212].

Field studies

There has been an improvement in the quantity and quality of ambient measurements that are helpful in evaluating both models and emission inventories. The offline measurement of SOA tracers in the field relies on suitable marker compounds being identified from laboratory experiments, however, the lack of identified ASOA tracers limits the understanding of ASOA abundance and variability.

A number of advanced instruments such as PILS-WSOC (Particle in Liquid Sampler—Water Soluble Organic Carbon)[213] AMS/ACSM (Aerosol chemical speciation monitor)[39,214], TAG-AMS (thermal desorption aerosol gas chromatograph-AMS)[215], EESI-TOF-MS (extractive electrospray ionization-time of flight-MS)[216–219], PTR-MS (proton-transfer reaction-MS) or CIMS (chemical ionization MS)[220], are available to quantify OM at a high time resolution (i.e., minutes or seconds). These techniques have been used in many field studies and are able to separate SOA from POA. The online techniques often reduce the likely errors that are introduced by filter-based measurements as the latter are performed over several hours to days, making it challenging to differentiate atmospheric processes. However, the deployment of these instruments for long periods is labour intensive and expensive. In addition, the identification of SOA from different sources may not be always possible as the mass fragments from the ionisation of molecules in mass spectrometry do not often represent a signature for a particular precursor or source. However, this is not always the case as instruments like CIMS or EESI-TOF-MS with good mass-resolution use softer ionization methods. Therefore, at present, the combination of available methods during field campaigns is highly recommended for a complete overview.

Modelling studies

There have been several improvements made in the parameterizations used for atmospheric modelling since the last decade, such as revisions in SOA yields of different precursors based on chamber studies under varying conditions and the use of a new framework (volatility basis set 'VBS' approach) to handle the complexities of SOA formation, reaction, and volatility in order to understand the thermodynamics of mixed inorganic-organic systems[4]. SOA formation has been represented using two approaches in the atmospheric models; empirical models (based on laboratory data)[221–223], and explicit/semi-explicit models (e.g., Master Chemical Mechanism)[224,225]. The heterogeneous reactions involving neutral to highly acidic aerosols are not very well accounted for in the existing SOA models. As a result, the current models mostly underestimate SOA mass in comparison with what is typically observed[7,201]. This could be also due to some missing SOA precursors, mostly anthropogenic, such as IVOCs and PAHs[27]. A modelling study, which attempted to parametrize SOA formation from alkanes and PAHs, showed 20–30% of total SOA produced from these precursors[226]. SVOCs or IVOCs are also not included in current emissions inventories and could be an important SOA precursor. In addition, the oxidation of existing POA or oxidation of semi-volatile SOA in the gas phase may enhance SOA formation from anthropogenic hydrocarbons. Bruns et al.[177] characterized primary and aged emissions from residential wood burning and showed that traditional SOA precursors account for only ~3–27% of the observed SOA, but ~84–116% of the SOA can be explained by including non-traditional precursors in models.

Overall, this discussion suggests that atmospheric models still require experimental data to parameterise SOA formation from different precursors, followed by evaluation using field data.

Integrated studies-laboratory/modelling/field

Despite rigorous research, several issues are emerging which can only be addressed via an integrated approach combining laboratory, field and modelling studies. For example, Xu et al.[227] combined all three approaches to investigate sources of OA and better constrain the OA budget. Their lab-in-the-field experiments reported that formed SOA from biogenic VOCs (α-pinene and β-caryophyllene) can be used as a proxy to apportion low oxygenated OA in the Southeastern US. In addition, their model also reproduces the magnitude and diurnal variability of low oxygenated OA measured at multiple sites in the Southeastern US. Their results also highlight that an integrated approach can facilitate the study of SOA formation under realistic atmospheric conditions, and improve atmospheric models which can be used on a large spatial scale to assess the sources of OA/SOA. Lamkaddam et al.[228] designed a study to investigate the aqueous-phase processing of isoprene oxidation products in cloud droplets using a similar approach. They integrate their experimental findings into a global model and reported that clouds significantly increase the amount of SOA. Similarly, Bruns et al.[177]. showed an improvement in the total SOA budget by including non-traditional precursors identified using laboratory experiments. Their findings suggest that identifying the main precursors responsible for SOA formation from residential wood burning enables improved model parameterizations for SOA contribution. However, such integrated studies are few and require more attention, especially those focusing on AVOCs.

CLOSING THOUGHTS

Significant advances have been made in the understanding of the formation and properties of ASOAs, but substantial gaps remain that present challenges for accurate characterization of the role of ASOAs in environmental degradation and climate. A better understanding of SOA chemical and physical properties is required to improve the modelling of global OA budgets. Thus, a major goal is to investigate/improve simulation of missing ASOA in atmospheric models through laboratory and field studies.

As outlined, in most of the studies reactions with OH are the dominant initial transformation pathway for AVOCs in the troposphere, although the importance of Cl reactions in the Arctic regions, marine and coastal areas have become apparent due to the rapid rate of reaction with SOA precursors. Additionally, reactions with NO_3 at night may represent a significant source of SOA and BrC formation in the atmosphere. Reaction pathways linked to Cl/NO_3 initiated oxidation of different AVOCs have not received as much attention and probably should be considered as a newly emerging focus of future research.

Another important line of research is the role of autoxidation reactions. The rapid autoxidation of RO_2 formed during VOC

oxidation results in HOMs that efficiently form SOA. However, most previous work is based on biogenic precursors (e.g., terpenes and sesquiterpenes)[229–231]. Therefore, although some knowledge has been developed for biogenic precursors, the following key questions remain:

What is the role of autoxidation in SOA formation from AVOCs?

How will it affect the SOA formation in urban environments where AVOC precursors dominate?

As the oxidation of aromatic hydrocarbons can rapidly form HOMs with extremely low volatility, it makes aromatic hydrocarbons a potential contributor to nucleation events observed in the urban environment[232,233]. There is a possibility that the study of these phenomena in highly pollutant environments may aid in discovering some new pathways for SOA formation chemistry.

Photochemical ageing of aerosols results in a change to aerosol composition and physical properties through various chemical and physical processes[234]. For example, UV-induced photodegradation can reduce the average size, mass and volatility distribution of SOA compounds resulting from photoinduced fragmentation and serve as a source of oxygenated VOCs[235,236]. This will cause SOA to scatter sunlight less efficiently, which in turn affects the Earth's climate. Alternatively, certain photochemical processes occurring on the surfaces of aerosol particles can also increase the average size and complexity of particulate organics[237]. Condensed-phase photochemical processes may produce a gaseous species comparable to its primary sources and could therefore measurably affect the budgets of both particulate and gaseous atmospheric organic compounds on a global scale. These processes are not fully characterised or accurately included in the global models. For example, Hodzic et al.[238] showed that the inclusion of condensed-phase photolysis in a global model can potentially result in ~50% of particle mass loss after 10 days of ageing with an assumption that condensed-phase photolysis of organics occurs at the same rate as in the gas-phase. Another recent combined experimental and modelling study also predicted about a 50% reduction in biogenic SOA due to SOA photodegradation[239]. This suggests the study of photochemical processes in the highly polluted environment through field campaigns, or of photochemical processes linked to AVOCs oxidation in the laboratory chambers can potentially aid in closing the SOA budget.

Finally, we conclude that our knowledge on SOA formation from AVOCs precursors is far from being complete. More integrated studies (laboratory/modelling/field) are needed to improve atmospheric models to capture the magnitude and variability of SOA to assess the impact on aerosol climate effects. Laboratory studies should include mixtures of precursors to simulate atmospheric conditions as closely as possible.

Received: 5 February 2021; Accepted: 7 February 2022;
Published online: 24 March 2022

REFERENCES

1. Boucher, O. et al. in *Climate Change 2013: The Physical Science Basis. Contribution of Working Group I to the Fifth Assessment Report of the Intergovernmental Panel on Climate Change* (eds Stocker, T.F. et al.) 571–657 (Cambridge University Press, 2013).
2. Brook, R. D. et al. Particulate matter air pollution and cardiovascular disease. *Circulation* **121**, 2331–2378 (2010).
3. Jathar, S. H. et al. Unspeciated organic emissions from combustion sources and their influence on the secondary organic aerosol budget in the United States. *Proc. Natl. Acad. Sci. USA* **111**, 10473–10478 (2014).
4. Kanakidou, M. et al. Organic aerosol and global climate modelling: a review. *Atmos. Chem. Phys.* **5**, 1053–1123 (2005).
5. Turpin, B. J. & Huntzicker, J. J. Identification of secondary organic aerosol episodes and quantitation of primary and secondary organic aerosol concentrations during SCAQS. *Atmos. Environ.* **29**, 3527–3544 (1995).
6. Zhang, Q. et al. Ubiquity and dominance of oxygenated species in organic aerosols in anthropogenically-influenced Northern Hemisphere midlatitudes. *Geophys. Res. Lett.* https://doi.org/10.1029/2007GL029979 (2007).
7. Hallquist, M. et al. The formation, properties and impact of secondary organic aerosol: current and emerging issues. *Atmos. Chem. Phys.* **9**, 5155–5236 (2009).
8. Guenther, A. et al. A global model of natural volatile organic compound emissions. *J. Geophys. Res.-Atmos.* **100**, 8873–8892 (1995).
9. Ziemann, P. J. & Atkinson, R. Kinetics, products, and mechanisms of secondary organic aerosol formation. *Chem. Soc. Rev.* **41**, 6582–6605 (2012).
10. Calvert, J. G. et al. *The Mechanisms of Atmospheric Oxidation of the Aromatic Hydrocarbons* (Oxford University Press, 2002).
11. Volkamer, R. et al. Secondary organic aerosol formation from anthropogenic air pollution: rapid and higher than expected. *Geophys. Res. Lett.* https://doi.org/10.1029/2006GL026899 (2006).
12. Stone, E. A., Hedman, C. J., Zhou, J., Mieritz, M. & Schauer, J. J. Insights into the nature of secondary organic aerosol in Mexico City during the MILAGRO experiment 2006. *Atmos. Environ.* **44**, 312–319 (2010).
13. Ding, X. et al. Tracer-based estimation of secondary organic carbon in the Pearl River Delta, south China. *J. Geophys. Res.* https://doi.org/10.1029/2011JD016596 (2012).
14. Volkamer, R., Ziemann, P. & Molina, M. Secondary organic aerosol formation from acetylene (C 2 H 2): seed effect on SOA yields due to organic photochemistry in the aerosol aqueous phase. *Atmos. Chem. Phys.* **9**, 1907–1928 (2009).
15. Blando, J. D. & Turpin, B. J. Secondary organic aerosol formation in cloud and fog droplets: a literature evaluation of plausibility. *Atmos. Environ.* **34**, 1623–1632 (2000).
16. Carlton, A. G., Wiedinmyer, C. & Kroll, J. H. A review of secondary organic aerosol (SOA) formation from isoprene. *Atmos. Chem. Phys.* **9**, 4987–5005 (2009).
17. Ervens, B., Turpin, B. J. & Weber, R. J. Secondary organic aerosol formation in cloud droplets and aqueous particles (aqSOA): a review of laboratory, field and model studies. *Atmos. Chem. Phys.* **11**, 11069–11102 (2011).
18. Mahilang, M., Deb, M. K. & Pervez, S. Biogenic secondary organic aerosols: a review on formation mechanism, analytical challenges and environmental impacts. *Chemosphere* **262**, 127771 (2021).
19. Edney, E. O. et al. Formation of Polyketones in irradiated toluene/propylene/NO x /air mixtures. *Aerosol Sci. Technol.* **35**, 998–1008 (2001).
20. Takekawa, H., Minoura, H. & Yamazaki, S. Temperature dependence of secondary organic aerosol formation by photo-oxidation of hydrocarbons. *Atmos. Environ.* **37**, 3413–3424 (2003).
21. Lim, Y. B. & Ziemann, P. J. Products and mechanism of secondary organic aerosol formation from reactions of n-alkanes with OH radicals in the presence of NOx. *Environ. Sci. Technol.* **39**, 9229–9236 (2005).
22. Lim, Y. B. & Ziemann, P. J. Chemistry of secondary organic aerosol formation from OH radical-initiated reactions of linear, branched, and cyclic alkanes in the presence of NOx. *Aerosol Sci. Technol.* **43**, 604–619 (2009).
23. Loza, C. L. et al. Secondary organic aerosol yields of 12-carbon alkanes. *Atmos. Chem. Phys.* **14**, 1423–1439 (2014).
24. Hunter, J. F., Carrasquillo, A. J., Daumit, K. E. & Kroll, J. H. Secondary organic aerosol formation from acyclic, monocyclic, and polycyclic alkanes. *Environ. Sci. Technol.* **48**, 10227–10234 (2014).
25. Ng, N. et al. Secondary organic aerosol formation from m-xylene, toluene, and benzene. *Atmos. Chem. Phys.* **7**, 3909–3922 (2007).
26. Presto, A. A., Miracolo, M. A., Donahue, N. M. & Robinson, A. L. Secondary organic aerosol formation from high-NOx photo-oxidation of low volatility precursors: n-Alkanes. *Environ. Sci. Technol.* **44**, 2029–2034 (2010).
27. Tkacik, D. S., Presto, A. A., Donahue, N. M. & Robinson, A. L. Secondary organic aerosol formation from intermediate-volatility organic compounds: cyclic, linear, and branched alkanes. *Environ. Sci. Technol.* **46**, 8773–8781 (2012).
28. Nguyen, T. B., Roach, P. J., Laskin, J., Laskin, A. & Nizkorodov, S. A. Effect of humidity on the composition of isoprene photooxidation secondary organic aerosol. *Atmos. Chem. Phys.* **11**, 6931–6944 (2011).
29. Hinks, M. L. et al. Effect of relative humidity on the composition of secondary organic aerosol from the oxidation of toluene. *Atmos. Chem. Phys.* **18**, 1643–1652 (2018).
30. Hildebrandt, L., Donahue, N. M. & Pandis, S. N. High formation of secondary organic aerosol from the photo-oxidation of toluene. *Atmos. Chem. Phys.* **9**, 2973–2986 (2009).
31. Fahnestock, K. A. S. et al. Secondary organic aerosol composition from C12 alkanes. *J. Phys. Chem.* **119**, 4281–4297 (2015).
32. Lamkaddam, H. et al. High-NOx photooxidation of n-Dodecane: temperature dependence of SOA formation. *Environ. Sci. Technol.* **51**, 192–201 (2017).
33. Lim, Y. B. & Ziemann, P. J. Effects of molecular structure on aerosol yields from OH radical-initiated reactions of linear, branched, and cyclic alkanes in the presence of NOx. *Environ. Sci. Technol.* **43**, 2328–2334 (2009).

34. Peng, Z. & Jimenez, J. L. Radical chemistry in oxidation flow reactors for atmospheric chemistry research. *Chem. Soc. Rev.* **49**, 2570–2616 (2020).
35. Li, K. et al. Secondary organic aerosol formation from α-pinene, alkanes, and oil-sands-related precursors in a new oxidation flow reactor. *Atmos. Chem. Phys.* **19**, 9715–9731 (2019).
36. Kang, E. Intorducing the concept of potential aerosol mass (PAM). *Atmos. Chem. Phys.* **7**, 5727–5744 (2007).
37. Lambe, A. T. et al. Transitions from functionalization to fragmentation reactions of laboratory secondary organic aerosol (SOA) generated from the OH oxidation of alkane precursors. *Environ. Sci. Technol.* **46**, 5430–5437 (2012).
38. Bertram, T. et al. A field-deployable, chemical ionization time-of-flight mass spectrometer. *Atmos. Chem. Phys.* **4**, 1471 (2011).
39. Jayne, J. T. et al. Development of an aerosol mass spectrometer for size and composition analysis of submicron particles. *Aerosol Sci. Technol.* **33**, 49–70 (2000).
40. Hamilton, J. F., Lewis, A. C., Reynolds, J. C., Carpenter, L. J. & Lubben, A. Investigating the composition of organic aerosol resulting from cyclohexene ozonolysis: low molecular weight and heterogeneous reaction products. *Atmos. Chem. Phys.* **6**, 4973–4984 (2006).
41. Flores, R. M. & Doskey, P. V. Evaluation of multistep derivatization methods for identification and quantification of oxygenated species in organic aerosol. *J. Chromatogr. A* **1418**, 1–11 (2015).
42. Schauer, J. J., Kleeman, M. J., Cass, G. R. & Simoneit, B. R. T. Measurement of emissions from air pollution sources. 4. C1−C27 organic compounds from cooking with seed oils. *Environ. Sci. Technol.* **36**, 567–575 (2002).
43. Ensberg, J. J. et al. Emission factor ratios, SOA mass yields, and the impact of vehicular emissions on SOA formation. *Atmos. Chem. Phys.* **14**, 2383–2397 (2014).
44. Atkinson, R., Arey, J. & Aschmann, S. M. Atmospheric chemistry of alkanes: review and recent developments. *Atmos. Environ.* **42**, 5859–5871 (2008).
45. Seinfeld, J. H.& Pandis, S. N. *Atmospheric Chemistry and Physics* (John Wiley & Sons, 2006).
46. Atkinson, R. & Arey, J. Atmospheric degradation of volatile organic compounds. *Chem. Rev.* **103**, 4605–4638 (2003).
47. Aimanant, S. & Ziemann, P. J. Chemical mechanisms of aging of aerosol formed from the reaction of n-Pentadecane with OH radicals in the presence of NOx. *Aerosol Sci. Technol.* **47**, 979–990 (2013).
48. Ruehl, C. R. et al. The influence of molecular structure and aerosol phase on the heterogeneous oxidation of normal and branched alkanes by OH. *J. Phys. Chem.* **117**, 3990–4000 (2013).
49. Reisen, F., Aschmann, S. M., Atkinson, R. & Arey, J. 1,4-Hydroxycarbonyl products of the OH radical initiated reactions of C5−C8 n-alkanes in the presence of NO. *Environ. Sci. Technol.* **39**, 4447–4453 (2005).
50. Yee, L. D. et al. Secondary organic aerosol formation from low-NOx photooxidation of Dodecane: evolution of multigeneration Gas-phase chemistry and aerosol composition. *J. Phys. Chem.* **116**, 6211–6230 (2012).
51. Craven, J. S. et al. Analysis of secondary organic aerosol formation and aging using positive matrix factorization of high-resolution aerosol mass spectra: application to the dodecane low-NOx system. *Atmos. Chem. Phys.* **12**, 11795–11817 (2012).
52. Yee, L. D. et al. Effect of chemical structure on secondary organic aerosol formation from C12 alkanes. *Atmos. Chem. Phys.* **13**, 11121–11140 (2013).
53. Ziemann, P. J. Formation of alkoxyhydroperoxy aldehydes and cyclic peroxyhemiacetals from reactions of cyclic alkenes with O3 in the presence of alcohols. *J. Phys. Chem.* **107**, 2048–2060 (2003).
54. Zhang, H. et al. OH-initiated heterogeneous oxidation of cholestane: a model system for understanding the photochemical aging of cyclic alkane aerosols. *J. Phys. Chem.* **117**, 12449–12458 (2013).
55. Zhang, X. et al. Role of ozone in SOA formation from alkane photooxidation. *Atmos. Chem. Phys.* **14**, 1733–1753 (2014).
56. Li, J. et al. Optical properties of secondary organic aerosols derived from long-chain alkanes under various NOx and seed conditions. *Sci. Total Environ.* **579**, 1699–1705 (2017).
57. Docherty, K. S. et al. Relative contributions of selected multigeneration products to chamber SOA formed from photooxidation of a range (C10–C17) of n-alkanes under high NOx conditions. *Atmos. Environ*. https://doi.org/10.1016/j.atmosenv.2020.117976 (2020).
58. Smith, D., Kleindienst, T. & McIver, C. Primary product distributions from the reaction of OH with m-, p-xylene, 1, 2, 4-and 1, 3, 5-trimethylbenzene. *J. Atmos. Chem.* **34**, 339–364 (1999).
59. Tsigaridis, K. & Kanakidou, M. Global modelling of secondary organic aerosol in the troposphere: a sensitivity analysis. *Atmos. Chem. Phys.* **3**, 1849–1869 (2003).
60. Bloss, C. et al. Evaluation of detailed aromatic mechanisms (MCMv3 and MCMv3.1) against environmental chamber data. *Atmos. Chem. Phys.* **5**, 623–639 (2005).
61. Atkinson, R. & Arey, J. Mechanisms of the gas-phase reactions of aromatic hydrocarbons and PAHS with OH and NO3 radicals. *Polycyclic Aromat. Compd.* **27**, 15–40 (2007).
62. Birdsall, A. W. & Elrod, M. J. Comprehensive NO-dependent study of the products of the oxidation of atmospherically relevant aromatic compounds. *J. Phys. Chem.* **115**, 5397–5407 (2011).
63. Ji, Y. et al. Reassessing the atmospheric oxidation mechanism of toluene. *Proc. Natl. Acad. Sci. U.S.A* **114**, 8169–8174 (2017).
64. Noda, J., Volkamer, R. & Molina, M. J. Dealkylation of alkylbenzenes: a significant pathway in the toluene, o-, m-, p-xylene + OH reaction. *J. Phys. Chem.* **113**, 9658–9666 (2009).
65. Aschmann, S. M., Arey, J. & Atkinson, R. Extent of H-atom abstraction from OH + p-cymene and upper limits to the formation of cresols from OH+m-xylene and OH+p-cymene. *Atmos. Environ.* **44**, 3970–3975 (2010).
66. Berndt, T., Böge, O. & Herrmann, H. On the formation of benzene oxide/oxepin in the gas-phase reaction of OH radicals with benzene. *Chem. Phys. Lett.* **314**, 435–442 (1999).
67. Bloss, C. et al. Development of a detailed chemical mechanism (MCMv3.1) for the atmospheric oxidation of aromatic hydrocarbons. *Atmos. Chem. Phys.* **5**, 641–664 (2005).
68. Forstner, H. J. L., Flagan, R. C. & Seinfeld, J. H. Secondary organic aerosol from the photooxidation of aromatic hydrocarbons: molecular composition. *Environ. Sci. Technol.* **31**, 1345–1358 (1997).
69. Bethel, H. L., Atkinson, R. & Arey, J. Products of the gas-phase reactions of OH radicals with p-Xylene and 1,2,3- and 1,2,4-trimethylbenzene: effect of NO2 concentration. *J. Phys. Chem.* **104**, 8922–8929 (2000).
70. Jang, M. & Kamens, R. M. Characterization of secondary aerosol from the photooxidation of toluene in the presence of NOx and 1-propene. *Environ. Sci. Technol.* **35**, 3626–3639 (2001).
71. Sato, K., Hatakeyama, S. & Imamura, T. Secondary organic aerosol formation during the photooxidation of toluene: NOx dependence of chemical composition. *J. Phys. Chem.* **111**, 9796–9808 (2007).
72. Volkamer, R., Platt, U. & Wirtz, K. Primary and secondary glyoxal formation from aromatics: experimental evidence for the bicycloalkyl−radical pathway from benzene, toluene, and p-xylene. *J. Phys. Chem.* **105**, 7865–7874 (2001).
73. Arey, J. et al. Dicarbonyl products of the OH radical-initiated reaction of a series of aromatic hydrocarbons. *Environ. Sci. Technol.* **43**, 683–689 (2009).
74. Zhao, J., Zhang, R., Misawa, K. & Shibuya, K. Experimental product study of the OH-initiated oxidation of m-xylene. *J. Photochem. Photobiol. A-Chem.* **176**, 199–207 (2005).
75. Song, C., Na, K., Warren, B., Malloy, Q. & Cocker, D. R. Secondary organic aerosol formation from the photooxidation of p- and o-Xylene. *Environ. Sci. Technol.* **41**, 7403–7408 (2007).
76. Wyche, K. P. et al. Gas phase precursors to anthropogenic secondary organic aerosol: detailed observations of 1,3,5-trimethylbenzene photooxidation. *Atmos. Chem. Phys.* **9**, 635–665 (2009).
77. Sato, K. et al. AMS and LC/MS analyses of SOA from the photooxidation of benzene and 1,3,5-trimethylbenzene in the presence of NOx: effects of chemical structure on SOA aging. *Atmos. Chem. Phys.* **12**, 4667–4682 (2012).
78. Pereira, K. L. et al. Insights into the formation and evolution of individual compounds in the particulate phase during aromatic photo-oxidation. *Environ. Sci. Technol.* **49**, 13168–13178 (2015).
79. Li, L., Tang, P., Nakao, S., Chen, C. L. & Cocker, D. R. III . Role of methyl group number on SOA formation from monocyclic aromatic hydrocarbons photooxidation under low-NOx conditions. *Atmos. Chem. Phys.* **16**, 2255–2272 (2016).
80. Zhang, P., Huang, J., Shu, J. & Yang, B. Comparison of secondary organic aerosol (SOA) formation during o-, m-, and p-xylene photooxidation. *Environ. Pollut.* **245**, 20–28 (2019).
81. Keyte, I. J., Harrison, R. M. & Lammel, G. Chemical reactivity and long-range transport potential of polycyclic aromatic hydrocarbons - a review. *Chem. Soc. Rev.* **42**, 9333–9391 (2013).
82. Shakya, K. M. & Griffin, R. J. Secondary organic aerosol from photooxidation of polycyclic aromatic hydrocarbons. *Environ. Sci. Technol.* **44**, 8134–8139 (2010).
83. Zhou, S. & Wenger, J. C. Kinetics and products of the gas-phase reactions of acenaphthylene with hydroxyl radicals, nitrate radicals and ozone. *Atmos. Environ.* **75**, 103–112 (2013).
84. Zhou, S. & Wenger, J. C. Kinetics and products of the gas-phase reactions of acenaphthene with hydroxyl radicals, nitrate radicals and ozone. *Atmos. Environ.* **72**, 97–104 (2013).
85. Kautzman, K. E. et al. Chemical composition of gas- and aerosol-phase products from the photooxidation of naphthalene. *J. Phys. Chem.* **114**, 913–934 (2010).
86. Riva, M., Robinson, E. S., Perraudin, E., Donahue, N. M. & Villenave, E. Photochemical aging of secondary organic aerosols generated from the photooxidation of polycyclic aromatic hydrocarbons in the gas-phase. *Environ. Sci. Technol.* **49**, 5407–5416 (2015).

87. Jobson, B. T. et al. Measurements of C2-C6hydrocarbons during the polar sunrise1992 experiment: evidence for Cl atom and Br atom chemistry. *J. Geophys. Res.* **99**, 25355–25368 (1994).
88. Ariya, P. A., Niki, H., Harris, G. W., Anlauf, K. G. & Worthy, D. E. J. Polar sunrise experiment 1995: hydrocarbon measurements and tropospheric Cl and Br-atoms chemistry. *Atmos. Environ.* **33**, 931–938 (1999).
89. Knipping, E. M. & Dabdub, D. Impact of chlorine emissions from sea-salt aerosol on coastal urban ozone. *Environ. Sci. Technol.* **37**, 275–284 (2003).
90. Atkinson, R. Gas-phase tropospheric chemistry of volatile organic compounds: 1. alkanes and alkenes. *J. Phys. Chem. Ref. Data* **26**, 215–290 (1997).
91. Riva, M. et al. Gas- and particle-phase products from the chlorine-initiated oxidation of polycyclic aromatic hydrocarbons. *J. Phys. Chem.* **119**, 11170–11181 (2015).
92. Wang, L., Arey, J. & Atkinson, R. Reactions of chlorine atoms with a series of aromatic hydrocarbons. *Environ. Sci. Technol.* **39**, 5302–5310 (2005).
93. Dhulipala, S. V., Bhandari, S. & Ruiz., L. H. Formation of oxidized organic compounds from Cl-initiated oxidation of toluene. *Atmos. Environ.* **199**, 265–273 (2019).
94. Wang, D. S. & Hildebrandt, L. Ruiz. Chlorine-initiated oxidation of n-alkanes under high-NOx conditions: insights into secondary organic aerosol composition and volatility using a FIGAERO–CIMS. *Atmos. Chem. Phys.* **18**, 15535–15553 (2018).
95. Holt, T., Atkinson, R. & Arey, J. Effect of water vapor concentration on the conversion of a series of 1,4-hydroxycarbonyls to dihydrofurans. *J. Photochem. Photobiol. A-Chem.* **176**, 231–237 (2005).
96. Shi, B. et al. Atmospheric oxidation of C10~14 n-alkanes initiated by Cl atoms: kinetics and mechanism. *Atmos. Environ.* **222**, 117166 (2020).
97. Mayorga, R. J., Zhao, Z. & Zhang, H. Formation of secondary organic aerosol from nitrate radical oxidation of phenolic VOCs: Implications for nitration mechanisms and brown carbon formation. *Atmos. Environ.* **244**, 117910 (2021).
98. Bolzacchini, E. et al. Gas-phase reaction of phenol with NO3. *Environ. Sci. Technol.* **35**, 1791–1797 (2001).
99. Xu, F. et al. Dioxin formations from the radical/radical cross-condensation of phenoxy radicals with 2-chlorophenoxy radicals and 2,4,6-trichlorophenoxy radicals. *Environ. Sci. Technol.* **44**, 6745–6751 (2010).
100. Strollo, C. M. & Ziemann, P. J. Investigation of the formation of benzoyl peroxide, benzoic anhydride, and other potential aerosol products from gas–phase reactions of benzoylperoxy radicals. *Atmos. Environ.* **130**, 202–210 (2016).
101. Olariu, R. I. et al. FT-IR product study of the reactions of NO3 radicals with ortho-, meta-, and para-Cresol. *Environ. Sci. Technol.* **47**, 7729–7738 (2013).
102. Finewax, Z., de Gouw, J. A. & Ziemann, P. J. Identification and quantification of 4-nitrocatechol formed from OH and NO3 radical-initiated reactions of catechol in air in the presence of NOx: implications for secondary organic aerosol formation from biomass burning. *Environ. Sci. Technol.* **52**, 1981–1989 (2018).
103. Finewax, Z., de Gouw, J. A. & Ziemann, P. J. Products and secondary organic aerosol yields from the OH and NO3 radical-initiated oxidation of resorcinol. *ACS Earth Space Chem.* **3**, 1248–1259 (2019).
104. Atkinson, R. & Arey, J. Atmospheric chemistry of gas-phase polycyclic aromatic hydrocarbons: formation of atmospheric mutagens. *Environ. Health Perspect.* **102**, 117–126 (1994).
105. Brüggemann, M. et al. Organosulfates in ambient aerosol: state of knowledge and future research directions on formation, abundance, fate, and importance. *Environ. Sci. Technol.* **54**, 3767–3782 (2020).
106. Surratt, J. D. et al. Effect of acidity on secondary organic aerosol formation from isoprene. *Environ. Sci. Technol.* **41**, 5363–5369 (2007).
107. Iinuma, Y., Müller, C., Böge, O., Gnauk, T. & Herrmann, H. The formation of organic sulfate esters in the limonene ozonolysis secondary organic aerosol (SOA) under acidic conditions. *Atmos. Environ.* **41**, 5571–5583 (2007).
108. Surratt, J. D. et al. Reactive intermediates revealed in secondary organic aerosol formation from isoprene. *Proc. Natl. Acad. Sci. USA* **107**, 6640–6645 (2010).
109. Iinuma, Y. et al. Evidence for the existence of organosulfates from β-pinene ozonolysis in ambient secondary organic aerosol. *Environ. Sci. Technol.* **41**, 6678–6683 (2007).
110. Surratt, J. D. et al. Evidence for organosulfates in secondary organic aerosol. *Environ. Sci. Technol.* **41**, 517–527 (2006).
111. Nozière, B., Ekström, S., Alsberg, T. & Holmström, S. Radical-initiated formation of organosulfates and surfactants in atmospheric aerosols. *Geophys. Res. Lett.* **37**, L05806 (2010).
112. Rudziński, K. J., Gmachowski, L. & Kuznietsova, I. Reactions of isoprene and sulphoxy radical-anions—a possible source of atmospheric organosulphites and organosulphates. *Atmos. Chem. Phys.* **9**, 2129–2140 (2009).
113. Passananti, M. et al. Organosulfate formation through the heterogeneous reaction of sulfur dioxide with unsaturated fatty acids and long-chain alkenes. *Angew. Chem. Int. Ed. Engl.* **55**, 10336–10339 (2016).
114. Huang, L., Coddens, E. M. & Grassian, V. H. Formation of organosulfur compounds from aqueous phase reactions of S(IV) with methacrolein and methyl vinyl ketone in the presence of transition metal ions. *ACS Earth Space Chem.* **3**, 1749–1755 (2019).
115. Surratt, J. D. et al. Organosulfate formation in biogenic secondary organic aerosol. *J. Phys. Chem. A* **112**, 8345–8378 (2008).
116. Tao, S. et al. Molecular characterization of organosulfates in organic aerosols from shanghai and Los Angeles urban areas by nanospray-desorption electrospray ionization high-resolution mass spectrometry. *Environ. Sci. Technol.* **48**, 10993–11001 (2014).
117. Kuang, B.-Y., P. Lin, M. Hu & J. Yu. Aerosol size distribution characteristics of organosulfates in the Pearl River Delta region, China. *Atmos. Environ*. https://doi.org/10.1016/j.atmosenv.2015.09.024 (2015).
118. Ng, N. L. et al. Secondary organic aerosol (SOA) formation from reaction of isoprene with nitrate radicals (NO3). *Atmos. Chem. Phys.* **8**, 4117–4140 (2008).
119. Mael, L. E., Jacobs, M. I. & Elrod, M. J. Organosulfate and nitrate formation and reactivity from epoxides derived from 2-methyl-3-buten-2-ol. *J. Phys. Chem. A* **119**, 4464–4472 (2015).
120. Zhang, H. et al. Organosulfates as tracers for secondary organic aerosol (SOA) formation from 2-Methyl-3-Buten-2-ol (MBO) in the atmosphere. *Environ. Sci. Technol.* **46**, 9437–9446 (2012).
121. Schindelka, J., Iinuma, Y., Hoffmann, D. & Herrmann, H. Sulfate radical-initiated formation of isoprene-derived organosulfates in atmospheric aerosols. *Faraday Discuss.* **165**, 237–259 (2013).
122. Safi Shalamzari, M. et al. Mass spectrometric characterization of organosulfates related to secondary organic aerosol from isoprene. *Rapid Commun. Mass Spectrom.* **27**, 784–794 (2013).
123. Shalamzari, M. S. et al. Characterization of polar organosulfates in secondary organic aerosol from the unsaturated aldehydes 2-E-pentenal, 2-E-hexenal, and 3-Z-hexenal. *Atmos. Chem. Phys.* **16**, 7135–7148 (2016).
124. Liggio, J. & Li, S.-M. Organosulfate formation during the uptake of pinonaldehyde on acidic sulfate aerosols. *Geophys. Res. Lett.* **33**, L13808 (2006).
125. Iinuma, Y., Boge, O., Kahnt, A. & Herrmann, H. Laboratory chamber studies on the formation of organosulfates from reactive uptake of monoterpene oxides. *Phys. Chem. Chem. Phys.* **11**, 7985–7997 (2009).
126. Chan, M. N. et al. Influence of aerosol acidity on the chemical composition of secondary organic aerosol from β-caryophyllene. *Atmos. Chem. Phys.* **11**, 1735–1751 (2011).
127. Riva, M. et al. Evidence for an unrecognized secondary anthropogenic source of organosulfates and sulfonates: gas-phase oxidation of polycyclic aromatic hydrocarbons in the presence of sulfate aerosol. *Environ. Sci. Technol.* **49**, 6654–6664 (2015).
128. Riva, M. et al. Chemical characterization of organosulfates in secondary organic aerosol derived from the photooxidation of alkanes. *Atmos. Chem. Phys.* **16**, 11001–11018 (2016).
129. Ma, Y., Xu, X., Song, W., Geng, F. & Wang, L. Seasonal and diurnal variations of particulate organosulfates in urban Shanghai, China. *Atmos. Environ.* **85**, 152–160 (2014).
130. Odum, J. R. et al. Gas/particle partitioning and secondary organic aerosol yields. *Environ. Sci. Technol.* **30**, 2580–2585 (1996).
131. Odum, J. R. et al. Aromatics, reformulated gasoline, and atmospheric organic aerosol formation. *Environ. Sci. Technol.* **31**, 1890–1897 (1997).
132. Lambe, A. T. et al. Transitions from functionalization to fragmentation reactions of laboratory secondary organic aerosol (SOA) generated from the OH oxidation of alkane precursors. *Environ. Sci. Technol.* **46**, 5430–5437 (2012).
133. Izumi, K. & Fukuyama, T. Photochemical aerosol formation from aromatic hydrocarbons in the presence of NOx. *Atmos. Environ.* **24**, 1433–1441 (1990).
134. Kleindienst, T. E. et al. Secondary organic aerosol formation from the oxidation of aromatic hydrocarbons in the presence of dry submicron ammonium sulfate aerosol. *Atmos. Environ.* **33**, 3669–3681 (1999).
135. Song, C., Na, K. & Cocker, D. R. Impact of the hydrocarbon to NOx ratio on secondary organic aerosol formation. *Environ. Sci. Technol.* **39**, 3143–3149 (2005).
136. Healy, R. M., Temime, B., Kuprovskyte, K. & Wenger, J. C. Effect of relative humidity on gas/particle partitioning and aerosol mass yield in the photooxidation of p-Xylene. *Environ. Sci. Technol.* **43**, 1884–1889 (2009).
137. Lu, Z., Hao, J., Takekawa, H., Hu, L. & Li, J. Effect of high concentrations of inorganic seed aerosols on secondary organic aerosol formation in the m-xylene/NOx photooxidation system. *Atmos. Environ.* **43**, 897–904 (2009).
138. Li, L., Tang, P., Nakao, S. & Cocker, D. R. III Impact of molecular structure on secondary organic aerosol formation from aromatic hydrocarbon photooxidation under low-NOx conditions. *Atmos. Chem. Phys.* **16**, 10793–10808 (2016).
139. Chen, L. et al. Ozone and secondary organic aerosol formation of toluene/NOx irradiations under complex pollution scenarios. *Aerosol. Air Qual. Res.* **17**, 1760–1771 (2017).

140. Chan, A. W. H. et al. Secondary organic aerosol formation from photooxidation of naphthalene and alkylnaphthalenes: implications for oxidation of intermediate volatility organic compounds (IVOCs). *Atmos. Chem. Phys.* **9**, 3049–3060 (2009).
141. Borrás, E. & Tortajada-Genaro, L. A. Secondary organic aerosol formation from the photo-oxidation of benzene. *Atmos. Environ.* **47**, 154–163 (2012).
142. Cocker, D. R., Mader, B. T., Kalberer, M., Flagan, R. C. & Seinfeld, J. H. The effect of water on gas–particle partitioning of secondary organic aerosol: II. m-xylene and 1,3,5-trimethylbenzene photooxidation systems. *Atmos. Environ.* **35**, 6073–6085 (2001).
143. Kamens, R. M. et al. Secondary organic aerosol formation from toluene in an atmospheric hydrocarbon mixture: water and particle seed effects. *Atmos. Environ.* **45**, 2324–2334 (2011).
144. Zhou, Y. et al. Secondary organic aerosol formation from xylenes and mixtures of toluene and xylenes in an atmospheric urban hydrocarbon mixture: water and particle seed effects (II). *Atmos. Environ.* **45**, 3882–3890 (2011).
145. Jia, L. & Xu, Y. Effects of relative humidity on ozone and secondary organic aerosol formation from the photooxidation of benzene and ethylbenzene. *Aerosol Sci. Technol.* **48**, 1–12 (2014).
146. Lamkaddam, H. et al. Role of relative humidity in the secondary organic aerosol formation from high-NOx photooxidation of long-chain alkanes: n-Dodecane case study. *ACS Earth Space Chem.* **4**, 2414–2425 (2020).
147. Jia, L. & Xu, Y. Different roles of water in secondary organic aerosol formation from toluene and isoprene. *Atmos. Chem. Phys.* **18**, 8137–8154 (2018).
148. Wang, Y., Luo, H., Jia, L. & Ge, S. Effect of particle water on ozone and secondary organic aerosol formation from benzene-NO2-NaCl irradiations. *Atmos. Environ.* **140**, 386–394 (2016).
149. Kroll, J. H., Chan, A. W. H., Ng, N. L., Flagan, R. C. & Seinfeld, J. H. Reactions of semivolatile organics and their effects on secondary organic aerosol formation. *Environ. Sci. Technol.* **41**, 3545–3550 (2007).
150. Liu, T. et al. Comparison of secondary organic aerosol formation from toluene on initially wet and dry ammonium sulfate particles at moderate relative humidity. *Atmos. Chem. Phys.* **18**, 5677–5689 (2018).
151. Liu, C. et al. Enhancement of secondary organic aerosol formation and its oxidation state by SO2 during photooxidation of 2-methoxyphenol. *Atmos. Chem. Phys.* **19**, 2687–2700 (2019).
152. Hurley, M. D. et al. Organic aerosol formation during the atmospheric degradation of toluene. *Environ. Sci. Technol.* **35**, 1358–1366 (2001).
153. Klotz, B. et al. OH-initiated oxidation of benzene Part II.Influence of elevated NO concentrations. *Phys. Chem. Chem. Phys.* **4**, 4399–4411 (2002).
154. Cao, G. & Jang, M. Secondary organic aerosol formation from toluene photooxidation under various NOx conditions and particle acidity. *Atmos. Chem. Phys. Discuss.* **2008**, 14467–14495 (2008).
155. Yang, Z. et al. Effects of NOx and SO2 on the secondary organic aerosol formation from the photooxidation of 1,3,5-trimethylbenzene: a new source of organosulfates. *Environ. Pollut.* **264**, 114742 (2020).
156. Nihill, K., Ye, Q., Majluf, F., Krechmer, J. & Kroll. J. Influence of the NO/NO2 ratio on oxidation product distributions under high-NO conditions. *Environ. Sci. Technol.* **55,** 6594–6601 (2021).
157. Liu, S., Jiang, X., Tsona, N. T., Lv, C. & Du, L. Effects of NOx, SO(2) and RH on the SOA formation from cyclohexene photooxidation. *Chemosphere* **216**, 794–804 (2019).
158. Kang, E., Toohey, D. W. & Brune, W. H. Dependence of SOA oxidation on organic aerosol mass concentration and OH exposure: experimental PAM chamber studies. *Atmos. Chem. Phys.* **11**, 1837–1852 (2011).
159. Donahue, N. M., Robinson, A. L., Stanier, C. O. & Pandis, S. N. Coupled partitioning, dilution, and chemical aging of semivolatile organics. *Environ. Sci. Technol.* **40**, 2635–2643 (2006).
160. McFiggans, G. et al. Secondary organic aerosol reduced by mixture of atmospheric vapours. *Nature* **565**, 587–593 (2019).
161. Chen, Y. et al. Effect of titanium dioxide on secondary organic aerosol formation. *Environ. Sci. Technol.* **52**, 11612–11620 (2018).
162. Matsunaga, A. & Ziemann, P. J. Gas-wall partitioning of organic compounds in a Teflon film chamber and potential effects on reaction Product and Aerosol Yield Measurements. *Aerosol Sci. Technol.* **44**, 881–892 (2010).
163. Zhang, X. et al. Influence of vapor wall loss in laboratory chambers on yields of secondary organic aerosol. *Proc. Natl. Acad. Sci. USA* **111**, 5802–5807 (2014).
164. Pierce, J. R. et al. Constraining particle evolution from wall losses, coagulation, and condensation-evaporation in smog-chamber experiments: optimal estimation based on size distribution measurements. *Aerosol Sci. Technol.* **42**, 1001–1015 (2008).
165. Krechmer, J. E., Day, D. A. & Jimenez, J. L. Always lost but never forgotten: gas-phase wall losses are important in all teflon environmental chambers. *Environ. Sci. Technol.* **54**, 12890–12897 (2020).
166. Loza, C. L. et al. Chemical aging of m-xylene secondary organic aerosol: laboratory chamber study. *Atmos. Chem. Phys.* **12**, 151–167 (2012).
167. Schauer, J. J. et al. Source apportionment of airborne particulate matter using organic compounds as tracers. *Atmos. Environ.* **30**, 3837–3855 (1996).
168. Robinson, A. L. et al. Rethinking organic aerosols: semivolatile emissions and photochemical aging. *Science* **315**, 1259–1262 (2007).
169. Schauer, J. J., Kleeman, M. J., Cass, G. R. & Simoneit, B. R. T. Measurement of emissions from air pollution sources. 2. C1 through C30 organic compounds from medium duty diesel trucks. *Environ. Sci. Technol.* **33**, 1578–1587 (1999).
170. Miracolo, M. A. et al. Photo-oxidation of low-volatility organics found in motor vehicle emissions: production and chemical evolution of organic arosol mass. *Environ. Sci. Technol.* **44**, 1638–1643 (2010).
171. Weitkamp, E. A., Sage, A. M., Pierce, J. R., Donahue, N. M. & Robinson, A. L. Organic aerosol formation from photochemical oxidation of diesel exhaust in a smog chamber. *Environ. Sci. Technol.* **41**, 6969–6975 (2007).
172. Presto, A. A. et al. Intermediate-volatility organic compounds: a potential source of ambient oxidized organic aerosol. *Environ. Sci. Technol.* **43**, 4744–4749 (2009).
173. Schauer, J. J., Fraser, M. P., Cass, G. R. & Simoneit, B. R. Source reconciliation of atmospheric gas-phase and particle-phase pollutants during a severe photochemical smog episode. *Environ. Sci. Technol.* **36**, 3806–3814 (2002).
174. Platt, S. M. et al. Secondary organic aerosol formation from gasoline vehicle emissions in a new mobile environmental reaction chamber. *Atmos. Chem. Phys.* **13**, 9141–9158 (2013).
175. Du, Z. et al. Comparison of primary aerosol emission and secondary aerosol formation from gasoline direct injection and port fuel injection vehicles. *Atmos. Chem. Phys.* **18**, 9011–9023 (2018).
176. Chen, T. et al. Important role of aromatic hydrocarbons in SOA formation from unburned gasoline vapor. *Atmos. Environ.* **201**, 101–109 (2019).
177. Bruns, E. A. et al. Identification of significant precursor gases of secondary organic aerosols from residential wood combustion. *Sci. Rep.* **6**, 27881 (2016).
178. Liu, T., Li, Z., Chan, M. & Chan, C. K. Formation of secondary organic aerosols from gas-phase emissions of heated cooking oils. *Atmos. Chem. Phys.* **17**, 7333–7344 (2017).
179. Liu, T. et al. Significant production of secondary organic aerosol from emissions of heated cooking oils. *Environ. Sci. Technol. Lett.* **5**, 32–37 (2018).
180. Takhar, M., Li, Y. & Chan, A. W. H. Characterization of secondary organic aerosol from heated-cooking-oil emissions: evolution in composition and volatility. *Atmos. Chem. Phys.* **21**, 5137–5149 (2021).
181. McDonald, B. C. et al. Volatile chemical products emerging as largest petrochemical source of urban organic emissions. *Science* **359**, 760–764 (2018).
182. Li, K. et al. Enhanced light scattering of secondary organic aerosols by multiphase reactions. *Environ. Sci. Technol.* **51**, 1285–1292 (2017).
183. Li, K. et al. Effects of gas-particle partitioning on refractive index and chemical composition of m-Xylene secondary organic aerosol. *J. Phys. Chem.* **122**, 3250–3260 (2018).
184. Li, J. et al. Temperature effects on optical properties and chemical composition of secondary organic aerosol derived from n-dodecane. *Atmos. Chem. Phys.* **20**, 8123–8137 (2020).
185. Zhang, W. et al. Effects of SO2 on optical properties of secondary organic aerosol generated from photooxidation of toluene under different relative humidity conditions. *Atmos. Chem. Phys.* **20**, 4477–4492 (2020).
186. Kroll, J. H. et al. Carbon oxidation state as a metric for describing the chemistry of atmospheric organic aerosol. *Nature Chemistry* **3**, 133–139 (2011).
187. Hildebrandt Ruiz, L. et al. Formation and aging of secondary organic aerosol from toluene: changes in chemical composition, volatility, and hygroscopicity. *Atmos. Chem. Phys.* **15**, 8301–8313 (2015).
188. Petters, M. D. & Kreidenweis, S. M. A single parameter representation of hygroscopic growth and cloud condensation nucleus activity. *Atmos. Chem. Phys.* **7**, 1961–1971 (2007).
189. Jimenez, J. et al. Evolution of organic aerosols in the atmosphere. *Science* **326**, 1525–1529 (2009).
190. Massoli, P. et al. Relationship between aerosol oxidation level and hygroscopic properties of laboratory generated secondary organic aerosol (SOA) particles. *Geophys. Res. Lett.* https://doi.org/10.1029/2011GL046687 (2010).
191. Petters, S. S., Kreidenweis, S. M., Grieshop, A. P., Ziemann, P. J. & Petters, M. D. Temperature- and humidity-dependent phase states of secondary organic aerosols. *Geophys. Res. Lett.* **46**, 1005–1013 (2019).
192. Saukko, E. et al. Humidity-dependent phase state of SOA particles from biogenic and anthropogenic precursors. *Atmos. Chem. Phys.* **12**, 7517–7529 (2012).
193. Koop, T., Bookhold, J., Shiraiwa, M. & Pöschl, U. Glass transition and phase state of organic compounds: dependency on molecular properties and implications for secondary organic aerosols in the atmosphere. *Phys. Chem. Chem. Phys.* **13**, 19238–19255 (2011).

194. Shiraiwa, M., Ammann, M., Koop, T. & Pöschl., U. Gas uptake and chemical aging of semisolid organic aerosol particles. *Proc. Natl. Acad. Sci. USA* **108**, 11003–11008 (2011).
195. Song, M. et al. Relative humidity-dependent viscosity of secondary organic material from toluene photo-oxidation and possible implications for organic particulate matter over megacities. *Atmos. Chem. Phys.* **16**, 8817–8830 (2016).
196. Vaden, T. D., Imre, D., Beranek, J., Shrivastava, M. & Zelenyuk., A. Evaporation kinetics and phase of laboratory and ambient secondary organic aerosol. *Proc. Natl. Acad. Sci. USA* **108**, 2190–2195 (2011).
197. Virtanen, A. et al. An amorphous solid state of biogenic secondary organic aerosol particles. *Nature* **467**, 824–827 (2010).
198. Cappa, C. D. & Wilson, K. R. Evolution of organic aerosol mass spectra upon heating: implications for OA phase and partitioning behavior. *Atmos. Chem. Phys.* **11**, 1895–1911 (2011).
199. Bruns, E. A. et al. Inter-comparison of laboratory smog chamber and flow reactor systems on organic aerosol yield and composition. *Atmos. Meas. Tech. Discuss.* **8**, 309–352 (2015).
200. Lambe, A. T. et al. Effect of oxidant concentration, exposure time, and seed particles on secondary organic aerosol chemical composition and yield. *Atmos. Chem. Phys.* **15**, 3063–3075 (2015).
201. Kroll, J. H. & Seinfeld, J. H. Chemistry of secondary organic aerosol: formation and evolution of low-volatility organics in the atmosphere. *Atmos. Environ.* **42**, 3593–3624 (2008).
202. Donahue, N. M., Kroll, J. H., Pandis, S. N. & Robinson, A. L. A two-dimensional volatility basis set—Part 2: diagnostics of organic-aerosol evolution. *Atmos. Chem. Phys.* **12**, 615–634 (2012).
203. Ahern, A. T. et al. Production of secondary organic aerosol during aging of biomass burning smoke from fresh fuels and its relationship to VOC precursors. *J. Geophys. Res.-Atmos.* **124**, 3583–3606 (2019).
204. Lim, C. Y. et al. Secondary organic aerosol formation from the laboratory oxidation of biomass burning emissions. *Atmos. Chem. Phys.* **19**, 12797–12809 (2019).
205. Tiitta, P. et al. Transformation of logwood combustion emissions in a smog chamber: formation of secondary organic aerosol and changes in the primary organic aerosol upon daytime and nighttime aging. *Atmos. Chem. Phys.* **16**, 13251–13269 (2016).
206. Stefenelli, G. et al. Secondary organic aerosol formation from smoldering and flaming combustion of biomass: a box model parametrization based on volatility basis set. *Atmos. Chem. Phys.* **19**, 11461–11484 (2019).
207. Gordon, T. D. et al. Secondary organic aerosol formation exceeds primary particulate matter emissions for light-duty gasoline vehicles. *Atmos. Chem. Phys.* **14**, 4661–4678 (2014).
208. Gordon, T. D. et al. Secondary organic aerosol production from diesel vehicle exhaust: impact of aftertreatment, fuel chemistry and driving cycle. *Atmos. Chem. Phys.* **14**, 4643–4659 (2014).
209. Šimpraga, M. et al. Unravelling the functions of biogenic volatiles in boreal and temperate forest ecosystems. *Eur. J. For. Res.* **138**, 763–787 (2019).
210. Browne, E. C., Wooldridge, P. J., Min, K. E. & Cohen, R. C. On the role of monoterpene chemistry in the remote continental boundary layer. *Atmos. Chem. Phys.* **14**, 1225–1238 (2014).
211. Alam, M. S. et al. Mapping and quantifying isomer sets of hydrocarbons (≥C12) in diesel exhaust, lubricating oil and diesel fuel samples using GC × GC-ToF-MS. *Atmos. Meas. Tech.* **11**, 3047–3058 (2018).
212. Riva, M. et al. Photochemical aging of secondary organic aerosols generated from the photooxidation of polycyclic aromatic hydrocarbons in the gas-phase. *Environ. Sci. Technol.* https://doi.org/10.1021/acs.est.5b00442 (2015).
213. Sullivan, A. P. et al. A method for on-line measurement of water-soluble organic carbon in ambient aerosol particles: results from an urban site. *Atmos. Sci.* https://doi.org/10.1029/2004GL019681 (2004).
214. Ng, N. L. et al. An aerosol chemical speciation monitor (ACSM) for routine monitoring of the composition and mass concentrations of ambient aerosol. *Aerosol Sci. Technol.* **45**, 780–794 (2011).
215. Williams, B. J. et al. The first combined thermal desorption aerosol gas chromatograph—aerosol mass spectrometer (TAG-AMS). *Aerosol Sci. Technol.* **48**, 358–370 (2014).
216. Qi, L. et al. One-year characterization of organic aerosol composition and sources using an extractive electrospray ionization time-of-flight mass spectrometer (EESI-TOF). *Atmos. Chem. Phys. Discuss.* **2020**, 1–34 (2020).
217. Lopez-Hilfiker, F. D. et al. An extractive electrospray ionization time-of-flight mass spectrometer (EESI-TOF) for online measurement of atmospheric aerosol particles. *Atmos. Meas. Tech.* **12**, 4867–4886 (2019).
218. Qi, L. et al. Organic aerosol source apportionment in Zurich using an extractive electrospray ionization time-of-flight mass spectrometer (EESI-TOF-MS)—Part 2: biomass burning influences in winter. *Atmos. Chem. Phys.* **19**, 8037–8062 (2019).
219. Stefenelli, G. et al. Organic aerosol source apportionment in Zurich using an extractive electrospray ionization time-of-flight mass spectrometer (EESI-TOF-MS) – Part 1: biogenic influences and day–night chemistry in summer. *Atmos. Chem. Phys.* **19**, 14825–14848 (2019).
220. Lopez-Hilfiker, F. D. et al. A novel method for online analysis of gas and particle composition: description and evaluation of a Filter Inlet for Gases and AEROsols (FIGAERO). *Atmos. Meas. Tech.* **7**, 983–1001 (2014).
221. Henze, D. et al. Global modeling of secondary organic aerosol formation from aromatic hydrocarbons: high-vs. low-yield pathways. *Atmos. Chem. Phys.* **8**, 2405–2420 (2008).
222. Schell, B., Ackermann, I. J., Hass, H., Binkowski, F. S. & Ebel, A. Modeling the formation of secondary organic aerosol within a comprehensive air quality model system. *J. Geophys. Res.* **106**, 28275–28293 (2001).
223. Andersson-Sköld, Y. & Simpson, D. Secondary organic aerosol formation in northern Europe:a model study. *J. Geophys. Res.* **106**, 7357–7374 (2001).
224. Johnson, D., Jenkin, M. E., Wirtz, K. & Martin-Reviejo, M. Simulating the formation of secondary organic aerosol from the photooxidation of toluene. *J. Environ. Chem.* **1**, 150–165 (2004).
225. Johnson, D., Jenkin, M. E., Wirtz, K. & Martin-Reviejo, M. Simulating the formation of secondary organic aerosol from the photooxidation of aromatic hydrocarbons. *J. Environ. Chem.* **2**, 35–48 (2005).
226. Pye, H. O. T. & Pouliot, G. A. Modeling the role of alkanes, polycyclic aromatic hydrocarbons, and their oligomers in secondary organic aerosol formation. *Environ. Sci. Technol.* **46**, 6041–6047 (2012).
227. Xu, L. et al. Experimental and model estimates of the contributions from biogenic monoterpenes and sesquiterpenes to secondary organic aerosol in the southeastern United States. *Atmos. Chem. Phys.* **18**, 12613–12637 (2018).
228. Lamkaddam, H. et al. Large contribution to secondary organic aerosol from isoprene cloud chemistry. *Sci. Adv.* **7**, eabe2952 (2021).
229. Richters, S., Herrmann, H. & Berndt., T. Highly oxidized RO2 radicals and consecutive products from the ozonolysis of three sesquiterpenes. *Environ. Sci. Technol.* **50**, 2354–2362 (2016).
230. Rissanen, M. P. et al. Effects of chemical complexity on the autoxidation mechanisms of endocyclic alkene ozonolysis products: from methylcyclohexenes toward understanding α-Pinene. *J. Phys. Chem.* **119**, 4633–4650 (2015).
231. Ehn, M. et al. Gas phase formation of extremely oxidized pinene reaction products in chamber and ambient air. *Atmos. Chem. Phys.* **12**, 5113–5127 (2012).
232. Yu, H. et al. Nucleation and growth of sub-3 nm particles in the polluted urban atmosphere of a megacity in China. *Atmos. Chem. Phys.* **16**, 2641 (2016).
233. Xiao, S. et al. Strong atmospheric new particle formation in winter in urban Shanghai, China. *Atmos. Chem. Phys.* **15**, 1769 (2015).
234. George, C., Ammann, M., D'Anna, B., Donaldson, D. J. & Nizkorodov., S. A. Heterogeneous photochemistry in the atmosphere. *Chem. Rev.* **115**, 4218–4258 (2015).
235. Henry, K. M. & Donahue, N. M. Photochemical aging of α-Pinene secondary organic aerosol: effects of OH radical sources and photolysis. *J. Phys. Chem.* **116**, 5932–5940 (2012).
236. Baboomian, V. J., Gu, Y. & Nizkorodov., S. A. Photodegradation of secondary organic aerosols by long-term exposure to solar actinic radiation. *ACS Earth Space Chem.* **4**, 1078–1089 (2020).
237. Rapf, R. J. & Vaida, V. Sunlight as an energetic driver in the synthesis of molecules necessary for life. *Phys. Chem. Chem. Phys.* **18**, 20067–20084 (2016).
238. Hodzic, A. et al. Organic photolysis reactions in tropospheric aerosols: effect on secondary organic aerosol formation and lifetime. *Atmos. Chem. Phys.* **15**, 9253–9269 (2015).
239. Zawadowicz, M. A. et al. Photolysis controls atmospheric budgets of biogenic secondary organic aerosol. *Environ. Sci. Technol.* **54**, 3861–3870 (2020).
240. Nehr, S. *Mechanistic Studies on the OH-Initiated Atmospheric Oxidation of Selected Aromatic Hydrocarbons* ((Jülich Forschungszentrum Jülich, 2012).

ACKNOWLEDGEMENTS

This work was supported by the Natural Environment Research Council (APHH-Beijing and SOA grants): NE/N007190/1 (AIRPOLL-Beijing), NE/S006699/1 (SOA).

AUTHOR CONTRIBUTIONS

Conceptualization R. M. H., Z. S., T. V. V.; formal analysis T. V. V., D. S.; funding acquisition R. M. H., Z. S., T. V. V.; investigation D. S., T. V. V.; methodology T. V. V., D. S., R. M. H.; project administration R. M. H., Z. S.; resources R. M. H., Z. S.; supervision R. M. H., Z. S.; validation T. V. V., D. S.; visualization D. S.; writing—original draft T. V. V., D. S.; writing—review and editing Z. S., S. T., R. M. H.

COMPETING INTERESTS

R. M. H. is co-editor-in-chief of *npj Climate and Atmospheric Science* and was not involved in the journal's review of, or decisions related to, this manuscript. The authors declare no competing interests.

ADDITIONAL INFORMATION

Correspondence and requests for materials should be addressed to Roy M. Harrison.

Reprints and permission information is available at http://www.nature.com/reprints

Publisher's note Springer Nature remains neutral with regard to jurisdictional claims in published maps and institutional affiliations.